Atmos. Chem. Phys. Discuss., doi:10.5194/acp-2016-265, 2016
Manuscript under review for journal Atmos. Chem. Phys.
Published: 8 April 2016

Fluorescent Biological Aerosol Particle Measurements at a Tropical High Altitude Site in Southern India during Southwest Monsoon Season

A. E. Valsan[1,*], R. Ravikrishna[2], C. V. Biju[3], C. Pöhlker[4], V. R. Després[5], J. A. Huffman[6], U. Pöschl[7], and S. S. Gunthe[1,**]

[1]EWRE Division, Department of Civil Engineering, Indian Institute of Technology Madras, Chennai – 600 036, India.

[2]Department of Chemical Engineering, Indian Institute of Technology Madras, Chennai – 600 036, India.

[3]Department of Civil Engineering, College of Engineering Munnar, PB.No:45, County Hills, Munnar – 685612, India.

[4]Biogeochemistry Department, Max Planck Institute for Chemistry, P. O. Box Number 3060, Mainz, Germany.

[5]Institute of General Botany, Johannes Gutenberg University, Mainz, Germany.

[6]Department of Chemistry and Biochemistry, University of Denver, 2190 E. Iliff Ave., Denver, CO, 80208, USA.

[7]Multiphase Chemistry Department, Max Planck Institute for Chemistry, P. O. Box 3060, Mainz, Germany

To whom correspondence should be addressed:

[*]Aswathy E. Valsan (aswathyerat@gmail.com)

[**]Sachin S. Gunthe (s.gunthe@iitm.ac.in)

Atmos. Chem. Phys. Discuss., doi:10.5194/acp-2016-265, 2016
Manuscript under review for journal Atmos. Chem. Phys.
Published: 8 April 2016

Abstract

Primary Biological Aerosol Particles (PBAPs) like fungal spores, bacteria, pollen, etc. are reported to constitute large fraction of the atmospheric aerosols. They are responsible for the spread of organisms and diseases throughout the biosphere and may impact atmospheric processes and the hydrological cycle by acting as ice nuclei (IN) and giant cloud condensation nuclei (CCN). Despite their importance in the biosphere and climate, continuous measurements of PBAPs in high time and size resolutions are not available for the Indian subcontinent. Here we report the first measurements of fluorescent biological aerosol particles (FBAPs) in India. The measurements were carried out using an ultraviolet aerodynamic particle sizer (UV-APS) in Munnar, a high altitude tropical site in southern India. The study was conducted for three consecutive months during the Southwest monsoon season (1.June.2014 – 21.August.2014), which is marked by heavy and persistent rainfall and strong Westerly/Southwesterly clean winds.

Averaged over the entire campaign arithmetic mean number and mass concentrations of coarse-mode FBAP (> 1 µm) were 0.02 cm^{-3} and 0.24 µg m^{-3}, respectively, which corresponded to ~2 and 6 % of total aerosol loading, respectively. Average FBAP number size distribution exhibited a peak at ~3 µm, which was most likely contributed by fungal spores, as supported by scanning electron microscope (SEM) images, and the results are consistent with previous studies made for FBAP. During eleven weeks of measurements the corresponding total (TAP) coarse mode particle number concentration was highly variable in contrast to the variability observed in FBAP number concentration. Averaged over the entire campaign the TAP number and mass concentrations were 1.8 cm^{-3} and 7.0 µg m^{-3}. The TAP and FBAP number concentrations measured at this site were strongly dependent on changes in wind direction and rainfall. During the period of continuous and persistent rainfalls the TAP and FBAP concentration exhibited very

Atmos. Chem. Phys. Discuss., doi:10.5194/acp-2016-265, 2016
Manuscript under review for journal Atmos. Chem. Phys.
Published: 8 April 2016

low concentration levels (1.3 cm^{-3} and 0.005 cm^{-3}, respectively) with no observed diurnal variations. Averaged over the entire campaign FBAP exhibited a moderately diurnal variation with highest concentration during early morning hours (~06:00 – 08:00 hrs). The campaign averaged FBAP number concentrations were shown to correlate with daily patterns of meteorological parameters and were positively correlated with relative humidity (RH; R^2=0.58), and negatively with temperature (R^2=0.60) and wind speed (R^2=0.60). We did not observe any significant positive correlation with precipitation as reported by previous researchers from selected areas. These measurement results confirms the fact that fraction of PBAPs to TAP is strongly dependent on size and location and thus may constitute significant proportion of total aerosol particles.

Atmos. Chem. Phys. Discuss., doi:10.5194/acp-2016-265, 2016
Manuscript under review for journal Atmos. Chem. Phys.
Published: 8 April 2016

1 Introduction

Aerosols are generally defined as a colloidal system of solid or liquid particles suspended in a gaseous medium (Fuzzi et al., 1997; Pöschl, 2005) and are ubiquitous in the Earth's atmosphere. The term "Primary Biological Aerosol Particles" (PBAPs; sometimes also referred as bioaerosols or biological aerosols), describes a subset of aerosol particles, i.e. the solid airborne particles originating from biological organisms, including viruses, pollen, microorganisms (bacteria, fungal spores, etc.) and, protozoa or algae, etc., together with fragments of biological materials such as animal dander, plant debris etc. (Artaxo and Hansson, 1995; Coz et al., 2010; Després et al., 2007, 2012; Elbert et al., 2007). Bioaerosols can range in size from a few nanometers to few hundred micrometers in aerodynamic diameter, D_a, (Coz et al., 2010; Després et al., 2012; Jones and Harrison, 2004; Matthias-Maser and Jaenicke, 1994) with viruses being the smallest in size amongst the PBAPs followed by bacterial and fungal spores, while pollen, and plant and animal fragments represent the largest in size. Depending upon size and ecosystem PBAPs can constitute 14 – 70% of total number of coarse mode particles and around 20 – 24 % of total mass of PM_{10} (particulate matter with size ≤10 μm; Elbert et al., 2007; Després et al., 2012; Pöschl et al., 2010; Huffman et al., 2012). Bioaerosols are present in the ambient atmosphere either as a single particle, or as agglomerates (Valsan et al., 2015) and exhibit a variety of shapes and morphological characteristics. Further, it is likely that the surface structure, ice nucleating proteins, and other characteristics influence substantially the heterogeneous ice nuclei formation at various temperature levels (Morris et al., 2004, 2014) and they can also act as giant cloud condensation nuclei (GCCN) thus affecting the hydrological cycle (Andreae and Rosenfeld, 2008; Möhler et al., 2007). Other bioaerosols like pollen or fungal spores are often using air as the transport medium for distribution and transfer of genetic material and thus can travel and get

Atmos. Chem. Phys. Discuss., doi:10.5194/acp-2016-265, 2016
Manuscript under review for journal Atmos. Chem. Phys.
Published: 8 April 2016

transported over large distances (Huffman et al., 2010; Elbert et al., 2007; Hallar et al., 2011; Burrows et al., 2009). A side effect of such a transport and distribution, however, is that they are produced and spread in large quantities and play an important role in public health as they can cause allergies. Pathogenic fungi have long been recognized as major threats to animal health and plants including crops severely jeopardizing the food security (Fisher et al., 2012 and references therein).

Since the last century numerous studies have been conducted in different parts of the world to understand the abundance and diversity of bioaerosols using various sampling and measurement techniques, however confining to traditional methods. The last decade has experienced a substantial development and application of advanced online and offline techniques for studying characteristic properties of bioaerosols in the field and laboratory (Fröhlich-Nowoisky, et al., 2009; DeLeon-Rodriguez et al., 2013; Prenni et al., 2009; Huffman et al., 2010, 2012, 2013; Schumacher et al., 2013; Pöhlker et al., 2012, 2013).

Instruments utilizing laser-induced fluorescence (LIF) have been frequently deployed to the field, enabling real-time characterization of the number size distribution of PBAPs in high time and size resolution. However, instruments based on LIF do not provide detailed information about PBAPs, but rather provide broadly categorized information due to a mixture of biological fluorophores, each detected with varying efficiency (Pohlker et al., 2012, 2013). Most FBAP measurements have shown that the dominant size range for PBAPs number size distribution is 1 – 4 μm with concentration varying within the factor of 10 (Gabey et al., 2011, 2013; Healy et al., 2014; Huffman et al., 2010, 2012, 2013; Saari et al., 2015; Schumacher et al., 2013; Toprak and Schnaiter, 2013; Yu et al., 2016). As studied and described by Huffman et al., (2010) based on long-term PBAP measurements in central Europe, the signal detected by UV-APS (Ultraviolet

Atmos. Chem. Phys. Discuss., doi:10.5194/acp-2016-265, 2016
Manuscript under review for journal Atmos. Chem. Phys.
Published: 8 April 2016

Aerodynamic Particle Sizer) in ambient settings was defined as Fluorescent Biological Aerosol Particles (FBAP), and the resulting quantification of FBAP was further discussed and it was concluded that FBAP represents an approximate lower limit of actual abundance of PBAPs present in the ambient air sampled by the UV-APS. Thus, for the consistency and simplicity we use the similar terminology as suggested by Huffman et al., (2010). Hence the term FBAP is used as a lower limit proxy for primary biological aerosol particles (PBAPs), biological aerosols, biological aerosol particles, bioaerosols and similar terms mentioned in this study.

Despite such instrumental advancements described above, the studies related to the quantification of bioaerosols and their role in climate and human health have been extremely limited in space and time. Particularly, for the Indian subcontinent, which constitute around ~18% of the world's total population, studies related to the bioaerosols are relatively few with spotty analysis performed only by traditional techniques (Bhati and Gaur, 1979; Chakraborty et al., 1998; Gangamma, 2014; Srivastava et al., 2012; Sharma and Rai, 2008; Pachauri et al., 2013; Valsan et al., 2015; Ansari et al., 2015; Adhikari et al., 2004). Thus, sources, abundance, and properties of bioaerosols, which are strongly dependent on location and season, remains poorly characterized over the Indian subcontinent and need to be addressed systematically.

Investigating and quantifying the role of bioaerosols over the Indian continent is not only important because of the scarcity in the literature but also due to its unique climatic condition experienced by the two Monsoon seasons associated with two distinct synoptic scale wind patterns. Indian agriculture is strongly dependent on the Southwest Monsoon, and is the largest livelihood provider in India and contributes a significant figure to the Gross Domestic Product (GDP). Therefore, it is very important to better understand and quantify the role of bioaerosols in cloud and precipitation formation during Monsoon and convective rainfall. The concentrations of fluorescent aerosol was shown to increase during and after rainfall in a semi-arid forest in the Western US (Huffman et al., 2013), but the same pattern was not observed in a similar study in the Amazon basin (Huffman et al, 2012). Thus, the bioaerosols emitted during monsoon season could potentially play an important role in cloud and precipitation formation as shown by Ansari et al. (2015). Additionally, bioaerosols over the Indian sub-continent can have a direct societal impact where huge set of population may directly get affected by the spread of diseases and covertly due to the loss in agricultural output.

Thus, studies involving characterization of bioaerosols using advanced techniques over this region are important to understand and quantify the impact of bioaerosols on regional biodiversity with larger implication towards human and ecosystem health. With this motivation we have deployed an UV-APS for the detection and measurement of number size distribution of PBAPs at a high-altitude site of Munnar in Western Ghats of southern tropical India during Southwest monsoon season for ~3 months. To our knowledge this study presents the first multi-month ambient measurement investigations involving UV-APS over the Indian subcontinent.

2 Methods

2.1 Site Description

Measurements were performed to sample the air masses (see section 2.2) from a high-altitude site (Munnar; 10.09°N, 77.06°E; 1605 m amsl – above mean sea level – Fig. 1) located in the Western Ghats just 90 km away as the crow flies from Arabian Sea in the Southern part of tropical India. The observational site is located on a hill with a valley towards the South and a small mountain towards the North surrounded by dense vegetation including tea gardens and Eucalyptus trees. Climatologically this region is classified as subtropical highland with dry winters and is listed as the Shola forest-grass ecosystem as defined in the land-use type

Atmos. Chem. Phys. Discuss., doi:10.5194/acp-2016-265, 2016
Manuscript under review for journal Atmos. Chem. Phys.
Published: 8 April 2016

terminology. The Western Ghats, one of the eight mountain ranges in India and identified as one of the hottest hot spots of biodiversity (Myers et al., 2000) in the world, originates near the border of Maharashtra and Gujarat running ~1600 km towards South, parallel to the Western coast through the states of Gujarat, Maharashtra, Karnataka, Kerala, and Tamilnadu ending at the Southern tip of India near Kaniyakumari. This mountain range separates the coastal plain from the Deccan plateau making Western coastal plain a narrow land strip with a maximum width of ~ 110 – 120 km, sandwiched between the Western Ghats and the Arabian Sea. During the SW Monsoon season (June – September) the Southwesterly moisture laden winds are intercepted by the Western Ghats causing persistent and heavy rainfall on the windward side of these mountains. This causes the wash out and wet deposition of the pollutants in the coastal strip (Kerala) emitted due to anthropogenic activities thus bringing clean marine influx with minimum impact of anthropogenic emissions (Satheesh and Srinivasan, 2002). Therefore, during this particular season this observational site can be regarded as relatively pristine as compared to any other operational high-altitude observatory/site in Indian tropical region (Shika et al., 2016).

2.2 General Meteorology

Southern India nominally experiences two Monsoon seasons, the Southwest monsoon (SW; June – September) and the Northeast monsoon (NE; November – January), which are strongly associated with the movement of Inter-Tropical Convergence Zone, the ITCZ (Kanawade et al., 2014). The SW monsoon winds are dominant during June to September bringing almost anthropogenically "clean" (not affected by human activities) marine influx over the continent from Arabian Sea when ITCZ moves Northwards reaching 30°N during July (Naja and Lal, 2002). These air masses originate over the Indian Ocean and travel thousands of kilometers over oceanic water, including Arabian Sea, before reaching the observational site. The Southward

Atmos. Chem. Phys. Discuss., doi:10.5194/acp-2016-265, 2016
Manuscript under review for journal Atmos. Chem. Phys.
Published: 8 April 2016

movement of ITCZ reaching up to equator is associated with NE monsoon, which is also marked as winter season in India occurring during October to January, when prevailing winds are predominantly blowing in NE direction. The measurement site of Munnar receives more than 85% of its annual rainfall during SW monsoon season and experiences scattered rainfall events during NE monsoon season. The detailed meteorological parameters measured during the field measurement campaign carried out during SW Monsoon season at Munnar are discussed below.

2.2 Real-time fluorescence measurement

The biological aerosol particles from a high-altitude relatively pristine site were measured using an UV-APS (TSI Inc. Model 3314; Serial Number: 71331023) as per the standard instructions given in the technical manual. The detailed description about the instrument including operating principles, field operation, data analysis protocol, and critical operational parameters are discussed elsewhere (Kanaani, et al., 2007, 2008; Agranovski et al., 2003, 2004, 2005; Brosseau et al., 2000; Huffman et al., 2010, 2012; Hairston et al., 1997).

Briefly, the instrument is capable of measuring the aerosol particles in aerodynamic diameter (D_a) range of 0.54 – 19.81 μm over 52 channels by means of measuring the time-of-flight between two He-Ne red lasers (λ=633 nm). Once the particle size is determined, the same particle is further excited using a third ultraviolet Nd:YAG laser (λ=355 nm) and emissions are measured in the range of 420 – 575 nm. The spectrally unresolved total fluorescence is recorded for each individual particle in to one of the 64 channels with increasing order of fluorescence intensity. Huffman et al., (2010) described that the counting efficiency of the instrument drops below 100% at D_a< 0.7 μm (counting efficiency ~50% at 0.54 μm), hence, the particle number concentration values reported for particle sizes of <0.7 μm are lower limit of the actual concentration of the air sample. During analysis presented in this paper the particles detected in the size range of 15 – 20 μm were included and the reported number concentration values should be considered as the lower limit of the actual values present in the air sample, due to limitations in the size calibration for particles of this size. The UV-APS measurement cycle was initiated with 5 minutes interval (including the full diameter range scan for 285 seconds and 15 seconds of back-scanning recording total of 22280 sampling points during entire measurement campaign) where air sample was drawn with a volumetric flow rate of 5 L min^{-1} (lpm) at ambient temperature and pressure. All the times reported in this study are local time pertaining to Indian Standard Time (IST; GMT+5:30).

The UV-APS was placed next to the window inside a room in the College of Engineering, Munnar, Kerala located on a hill. A stain-less steel tubing with ¾" OD (outer diameter) and TSP inlet was used to construct the inlet unit for air sampling, which was ~9 m and ~2 m above the ground and rooftop, respectively. Thus the sampled air masses were expected to have minimal influence caused by the dynamics associated with the building structure. To minimize the particle losses due to impaction resulting from sharp bends, the electrically conductive silicon rubber tubing (~1.5 m; 12 mm inner diameter) was attached to the stain-less steel tube just outside the window (Fig. S1) avoiding the sharp bends. Before the sampled air was passed to the instrument, diffusion dryer (~1 m) with silica gel (orange color indicating) was used to dry and maintain the relative humidity <40%. Thus combining all the tubing involved in the air sampling the sample flow residence time was calculated to be ~ 20 seconds. The sample flow through all the tubing was expected to be laminar during entire sampling period and hence diffusion losses are expected to be negligible for all the size-ranges of the sampled particles.

For the present study we derived number size distribution of fluorescence biological aerosol particles, $dN_F/d\log D_a$, for each size bin by summing up the particle number concentration from

Atmos. Chem. Phys. Discuss., doi:10.5194/acp-2016-265, 2016
Manuscript under review for journal Atmos. Chem. Phys.
Published: 8 April 2016

the fluorescence channel numbers 3 – 64 and similarly the total particle number size distribution, dN_T/dlog D_a, was derived from channel numbers 1 – 64. In the present study we have used 1.0 µm as a cut-off diameter for given dN_F/dlog D_a and dN_T/dlog D_a to calculate the fluorescence biological aerosol number and total aerosol number concentrations, N_F and N_T, respectively. This is mainly due to the fact that particle counting efficiency of the UV-APS drops below unity at 0.7 µm and the interferences due to fluorescence from non-biological aerosol particles below 1.0 µm can at times be very high (Huffman et al., 2010). Also note that the cutoff at 1 µm moreover represents the border between fine (<1µm) and coarse (>1µm) modes of the particle number size distribution. The subscripts throughout this manuscript text "F" and "T" refer to fluorescent and total coarse mode particles, respectively. Please refer to Table 1 for the abbreviations, notations, and symbols used in this manuscript. The particle mass size distributions (dM/dlogD_a) for total as well as fluorescent biological aerosol particles were calculated for each size bin by multiplying dN/dlogD_a with volume of an aerodynamically equivalent sphere with the geometric midpoint diameter ($D_{a,g}$) and assuming the unit density (1 g cm^{-3}) and unit shape factor. The integral mass concentrations of coarse fluorescent biological aerosol particles and total coarse particles, M_F and M_T, respectively were calculated by integrating the particle mass distribution for D_a >1µm; but should be viewed as first approximation as a result of uncertainty associated with the density and shape of the particles (Huffman et al., 2010).

Fluorescence of submicron particles

It has been reported by previous researchers that UV-APS is known to exhibit fluorescence for some fraction of non-biological aerosol particles including soot, PAHs, and cigarettes smoke, which could be erroneously counted as FBAP (Huffman et al., 2010; Pan et al., 1999a, 1999b). It has also been emphasized that such interference can mostly occur for particles less than 1 µm as the contribution from combustion sources at this size range is expected to be dominant. To investigate the contribution of non-biological aerosol particles that are counted as fluorescence biological aerosol particles, Huffman et al., (2010) performed the correlation between the integrated number concentrations of fluorescent particles (N_F) and total particles (N_T) for different diameter ranges (only for the fluorescence channels >3). They found that the correlation for the submicron particles was systematically linear, whereas the correlation for supermicron particles was more random, indicating that a large fraction of submicron particles showing fluorescence might have been originated from anthropogenic sources, which may not be the case for the supermicron particles. To investigate the influence of anthropogenic emissions on submicron particles we performed the similar correlation analysis for the entire campaign and, however, found the different results. The correlation between integrated number concentrations of fluorescent particles (N_F) and total particles (N_T) for supermicron (D_a>1) and submicron (D_a<1 µm) diameter range exhibited a very poor scatter (R^2=0.03 and R^2=0.002 respectively; N=22280; Figs. S2) indicating extremely small percentage of fluorescence was contributed by non-biological aerosol particles in supermicron and submicron particle ranges.

Since certain component of the mineral dust may exhibit a weak fluorescence (Huffman et al., 2010; Sivaprakasam et al., 2004; Toprak and Schnaiter, 2013), we performed the separate correlation analysis for a focus period, which was dominated by the transport of mineral dust from West Asia, North Africa, and Arabian region (discussed below). The correlation between integrated number concentrations of N_F and N_T for D_a>1 µm was moderately linear (R^2=0.26; N=3138; Fig. S3a) compared to submicron size range during the dusty period (R^2=0.007; N=3138; Fig. S3b). As a result, correlation between N_F and N_T indicates that fraction of

Atmos. Chem. Phys. Discuss., doi:10.5194/acp-2016-265, 2016
Manuscript under review for journal Atmos. Chem. Phys.
Published: 8 April 2016

supermicron particles exhibiting fluorescence may have been contributed by mineral dust, but this being not the case for submicron particles.

From these analyses we infer that the contribution of non-biological aerosol particles exhibiting fluorescence was negligible in both submicron and supermicron (except during “dusty period”; discussed below) size ranges. Thus we hypothesize that due to persistent rainfall the submicron and supermicron particles resulted from combustion and other similar activities, were either efficiently removed or were not transported to the observational site, indicating that substantial fraction of the particles in both the size ranges were of biological origin. Thus this observational site could be potentially termed as relatively pristine and free from anthropogenic emissions during the monsoon season.

Please note, however, that to have the consistency and uniformity in the comparison of N_F, N_T, and other similar parameters reported by the previous studies we derived all the statistics associated with $dN_F/\text{dlog } D_a$ and $dN_T/\text{dlog } D_a$ with a cutoff diameter of 1 µm.

2.3 Meteorological parameter measurement

The meteorological parameters in parallel with the UV-APS measurements were recorded during the entire campaign using an ultrasonic weather sensor (Lufft WS600-UMB) installed on a rooftop at the same height and a few meters away from the UV-APS inlet (Fig. S1). The weather station was capable of recording temperature, dew point temperature, relative humidity, precipitation intensity, wind speed, wind direction, and air pressure and was set to record these meteorological parameters with every 5 minutes interval with time synchronized to UV-APS measurement clock. The data from the weather sensor was stored by using an in-house developed external data logger. The obtained meteorological data was compared with another ultrasonic weather station installed within the close vicinity (Valsala make). The scatter plots between the data (10 min averaged) obtained from our weather station and the one installed in the close vicinity exhibited very strong agreement for all the meteorological parameters measured/recorded (average $R^2 \geq 0.95$).

2.4 SEM Analysis

The samples for Scanning Electron Microscopy (SEM) analysis were collected on a 25 mm Nucleopore® Polycarbonate filter paper with pore sizes of 5 µm and 0.2 µm using a two stage filtering method as described by Valsan et al., (2015). All samples were collected for approximately a duration of 60 min at an average flow rate of 5 lpm and were stored in air-tight container at 4°C until SEM analysis. The five samples collected during the entire campaign were analyzed using two different scanning electron microscopes. 1. Quanta FEG 200 located at the Sophisticated Analytical Instrument Facility (SAIF) and 2. Hitachi S 4A00 located at the Chemical Engineering Department of Indian Institute of Technology Madras. Before loading the filter paper on to the studs, they were cut into small squares of ~1 cm^2 and sputter coated with gold particles. The biological aerosol particles were identified purely based on their morphological features adopting the method suggested by Matthias-Maser and Jaenicke (1991,1994). Detailed description on sample collection and analysis was discussed elsewhere (Valsan et al., 2015).

3 Results and discussions

3.1 Campaign overview

Figure 2 shows the temporal evolution and variability of the several parameters characteristic for the meteorological conditions, FBAP, and TAP properties observed throughout the measurement campaign during SW monsoon season at a high-altitude site of Munnar.

Atmos. Chem. Phys. Discuss., doi:10.5194/acp-2016-265, 2016
Manuscript under review for journal Atmos. Chem. Phys.
Published: 8 April 2016

Overall the meteorological conditions during the campaign at Munnar can be summarized as follows: The predominant wind direction was observed to be Westerly/Southwesterly (Fig. 1), which characterizes the monsoon season bringing almost anthropogenically clean marine influx (Vinoj and Satheesh, 2003) over the continent marked by presence of persistent rainfall, high relative humidity (RH), higher wind speeds, and lower temperatures. During this period the diurnal variations in temperature and relative humidity were totally absent and temperatures almost approached the dew point temperature. Further, the Westerly/Southwesterly air masses arriving at the observational site were free from any anthropogenic influence and were laden with dust and sea salt particles (Satheesh and Srinivasan, 2002; Vinoj et al., 2014; Prospero, 1979). On few occasions, however, Northerly winds were also observed, which was associated with calm winds, lower RH levels, higher temperatures, and reduced rainfall. During Northerly winds the temperature exhibited relatively more pronounced diurnal variations compared to the relative humidity. The average meteorological parameters (arithmetic mean±standard deviation) recorded during entire measurement period were: (840±1.3) hPa absolute pressure, (17.2±1.4)^{o}C ambient temperature, (96.4±5.7) % relative humidity, (2.8±1.3) m s^{-1} local wind speed, (270)° local wind direction (vector mean weighted by wind speed), and (4188) mm of accumulated rainfall.

The total of more than five months of bioaerosol measurements in high time and size resolution were performed at this site comprising two contrasting seasons, monsoon (dominated by Southwesterly winds) and winter (dominated by Northeasterly winds). In this study we present the results from the field campaign carried out during the SW monsoon season whereas the detailed results from the winter campaign from the same measurement site will be presented in the follow up study. We first discuss the characteristic features of the time series as a broad overview of the observed concentration levels, variability, and trends in N_T and N_F. Figure 2 (f,g,h,i,j) shows time series of geometric mean diameter (D_g), N_F, N_F/N_T, N_T, FBAP and TAP 3-D and the size distribution measured with the UV-APS for the entire campaign.

Throughout the measurement period the hourly averaged D_g time series consistently remained in the range of ~2 – 4 µm with almost no diurnal variations. During the second half of the campaign, the D_g, however, exhibited relatively high variability with average mean diameter of 2.6±0.7 µm. Unlike the N_T and N_F the variability in D_g was observed to be not affected by meteorological parameters except for wind direction (see section 3.6.1) on few occasions. The total coarse particle number concentration, N_T, exhibited high and consistent variability during entire measurement period, however, with no distinct diurnal cycle. Averaged (arithmetic mean±standard deviation) over the entire measurement period N_T was observed to be 1.8±1.5 cm^{-3} with lowest and highest concentrations of 0.01 cm^{-3} and 8.6 cm^{-3}, respectively. The average N_T concentration during the months of June, July, and August was 2.7±1.9 cm^{-3}, 1.5±0.96 cm^{-3}, and 0.96±0.77 cm^{-3}, respectively, with highest and lowest values for individual months respectively as follows: June: 8.6 and 0.04 cm^{-3}, July: 5.1 and 0.02 cm^{-3}, and August: 3.6 and 0.01 cm^{-3} (Fig. S4). The monthly averaged N_T concentration exhibited the decreasing trend from June to August as the monsoon progressed (Tab. 2). In contrast to the total aerosol particle number concentration, N_F, exhibited less pronounced but episodic peaks in the time series during majority of the measurement period resulting in modest variability and campaign arithmetic mean value was 0.02±0.02 cm^{-3}. The highest N_F concentration of ~0.52 cm^{-3} was observed on 3rd of June (and few more occasions) whereas the lowest N_F concentration was consistently observed on more than one occasion during the months of July and August. The average N_F

Atmos. Chem. Phys. Discuss., doi:10.5194/acp-2016-265, 2016
Manuscript under review for journal Atmos. Chem. Phys.
Published: 8 April 2016

concentration during June and August was 0.03±0.03 cm^{-3} and 0.015±0.02 cm^{-3}, respectively with lowest N_F concentration of 0.007±0.006 cm^{-3} in July (Tab. 2).

The time series of relative contribution of FBAP to TAP number, N_F/N_T, most of the time during campaign exhibited the similar temporal variability to N_F. The pronounced extreme values of N_F/N_T observed on few occasions resulted from strong variability in the concentrations of N_T rather than resulting from the variations in the concentrations of N_F, indicating the inverse correlation between N_T and N_F/N_T. Huffman et al., (2010) have also reported the similar inverse correlation between N_T and N_F/N_T from the measurements carried out at a semi-urban site from central Europe. Temporal evolution of N_F, N_F/N_T, and 3-D number size distribution for individual campaign months is shown in Fig. S5. A campaign overview of FBAP mass concentrations and 3-D size distribution for each five minutes of UV-APS sample averaged over the entire measurement period and individual months are shown in Figure S6. During the first month of measurement campaign M_F exhibited high concentration with sporadic spikes at irregular intervals with broader size distribution (~2 – 8 μm) towards the end of the month (with highest concentration ~ 6.0 μg m^{-3}). As the measurement campaign progressed, with arrival of persistent and heavy rainfall (whole of July and first-half of August) M_F exhibited a gradual decrease with minimum value reaching as low as 6 x 10^{-4} μg m^{-3}. After a period of consistent low mass concentration, during the last week of measurement campaign, M_F exhibited an increase with highest mass concentration of ~ 5.8 μg m^{-3}, which coincided with reduced and scattered rainfall.

3.2 Particle number and mass concentrations

3.2.1 Statistical distribution of number concentrations

Statistical distribution of five-minute number concentration measurements carried out at Munnar over the course of the campaign are shown in Fig. 3 and tabulated in Tab. 2. Over the entire

Atmos. Chem. Phys. Discuss., doi:10.5194/acp-2016-265, 2016
Manuscript under review for journal Atmos. Chem. Phys.
Published: 8 April 2016

measurement period the monthly mean of N_T varied by a factor ~3 from minimum in August (0.96 cm^{-3}) to a maximum in June (2.7 cm^{-3}). In addition to the highest concentration, the variability of N_T was also found to be highest in the month of June as can be seen from the size of the 5 – 95th percentile bars in Fig. 3a. The relative high variability in N_T for entire measurement period was largely contributed by the variability in N_T observed in the month of June. During the initial phase of Southwest monsoon season the predominant Westerly/Southwesterly winds are known to transport the mineral dust, which constitute large fraction of coarse mode (also in larger diameter size of fine mode fraction) TAP concentration, over the continental region **(**Vinoj et al., 2010, 2014; Li and Ramanathan, 2002; Satheesh and Srinivasan, 2002; Vinoj and Satheesh, 2003). As the monsoon progresses the persistent rainfall can cause the washout of these dust particles along the path of monsoonal rain, thus reducing the coarse mode TAP concentration (Pranesha and Kamra, 1997a,b; Radke et al., 1980; Moorthy et al., 1991). The monthly arithmetic mean and median average of N_T did not exhibit significant differences. The monthly mean values of N_F varied by the factor of ~4 with consistently high variability during all the observational months. Similar to N_T, the monthly mean average value and variability in N_F was highest in the month of June, with mean of 0.03±0.03 cm^{-3} and high size of 95th percentile (with value of 0.086 cm^{-3}), respectively. The lowest average concentration in N_F (0.007±0.006 cm^{-3}) observed in the month of July was associated with relatively lower variability as compared to other months of field measurement campaign. Unlike N_T, the arithmetic mean and median average of N_F for individual months exhibited a significant difference as can be seen from the box plot shown in Fig. 3b. The variability of N_F/N_T showed the similar temporal pattern as that of N_F, except that campaign average mean N_F concentration was higher than that of the August, whereas the campaign averaged mean N_F/N_T was observed to

Atmos. Chem. Phys. Discuss., doi:10.5194/acp-2016-265, 2016
Manuscript under review for journal Atmos. Chem. Phys.
Published: 8 April 2016

be lower than the mean calculated for August. As can be seen from Fig. 3c, the mean relative contribution of N_F to N_T was lowest in the month of July (~1%) and highest in the month of June and August (~3%). The median and mean for N_F/N_T, over the course of campaign were ~1 and 2%, respectively. The average values of N_F/N_T over this part of the globe were found to be lower as compared to previously investigated sites (Huffman et al., 2010, 2012; Bowers et al., 2009; Schumacher et al., 2013; Matthias-Maser and Jaenicke, 1995; Matthias-Maser et al., 2000; Gabey et al., 2010).

Diurnal patterns of the number concentration

The average diurnal trends for three individual months and the entire measurement campaign were analyzed. Figure 4 shows the median FBAP values for each hour of the day for three individual months and entire campaign, and Fig. S7 shows the corresponding TAP plots. Overall N_F exhibited a moderately diurnal pattern with consistent early morning (06:00 hr) peak at ~3 μm (Fig. 4a) where in the month of July this early morning peak was absent. A relatively weak peak during late evening (20:00 hr) in FBAP concentration at ~3 μm was consistently observed in the month of July. In the month of June the average diurnal N_F concentration started increasing early in the evening (~18:00 hr), which gradually increased through the night and reaching maximum at ~06:00 hr and started decreasing thereafter as day progressed. The average diurnal N_F pattern in August exhibited more or less qualitatively similar features to that of diurnal pattern observed in June. In general the weak diurnal pattern observed in N_F during the month of July was consistent with weak RH and temperature diurnal patterns, and persistent rainfall observed during July. The early morning peak at ~3 μm on the diurnal scale was also reported from pristine Amazonian rainforest environment (Huffman et al., 2012). Corresponding average size distributions for entire measurement period will be discussed in details in Sec. 3.3. The diurnal

Atmos. Chem. Phys. Discuss., doi:10.5194/acp-2016-265, 2016
Manuscript under review for journal Atmos. Chem. Phys.
Published: 8 April 2016

variations of N_T (Fig. S7), on the other hand were very distinct from those of N_F. The size resolved dN_T/dlog D_a for each individual months exhibited a consistent and flat concentration profile at <1 μm, except for the month of August where a pronounced afternoon peak (~12:00) at ~1 μm was observed. Reduced rainfall and substantial changes in meteorological parameters including the change in prevailing wind speed and shift in direction during later half of August might have caused the appearance of afternoon peak due to particles resulting from local sources. As like N_F, N_T showed the strong quantitative variability amongst each individual month (Fig. S7). Previous studies where similar instrument was used have reported that pronounced diurnal variations in N_T are strongly coupled with diurnal variations in meteorological variables especially mixing layer depth (Garland et al., 2009; Raatikainen et al., 2014; Du et al., 2013). The absence of pronounced diurnal variations in N_T at this particular site may be a result of weak dependence of coarse mode TAP concentrations on meteorological parameters combined with persistent rainfall causing the washout of these particles (Radke et al., 1980; Raatikainen et al., 2014; Kanawade et al., 2014; Shika et al., 2016). This also indicates the absence of any strong and localized source of anthropogenic emissions during most of the campaign period. Diurnal patterns of N_F/N_T more or less followed the same pattern as that of N_F during all the measurement months owing to complete absence of diurnal variability in N_T. Averaged over the entire campaign the N_F/N_T was found to be highest during early morning hour at ~06:00 hr (~3.2%) consistent with the time of high N_F concentration (Fig. 4). The distinct diurnal pattern in N_F and N_T supports the fact that the sources of TAP and FBAP were different over this region.

3.2.2 Statistical distribution of mass concentration

Basically UV-APS measures the particle number; the average mass of size-resolved particles can be derived as first approximation by assuming the particle density equal to 1 g cm^{-3} (unit density). Accordingly the overview of mass concentration of FBAP over the course of measurement period is presented here. The statistical distribution of five minutes mass concentration derived from number concentration measurements over the course of campaign is shown in Fig. 5 and tabulated in Tab. 2. The monthly mean values of M_T exhibited the similar trend and temporal variability as that of N_T with overall decrease in M_T through the course of measurement months as campaign progressed. The highest monthly average concentration of M_T (~10.6 µg m^{-3}) was observed in the month of June whereas the lowest M_T of ~4.2 µg m^{-3} was observed in the month of August. Averaged over the entire measurement period the mean M_T at Munnar was ~7 µg m^{-3}, which was comparable to the values reported from central European city (M_T ~7.3 µg m^{-3}) and higher than concentration of M_T (~2.5 µg m^{-3}) reported from pristine Amazonian rainforest region measured during wet season (Huffman et al., 2010; 2012). The monthly mean values of M_F, on the other hand, did not exhibit similar pattern like M_T, but followed temporal pattern like N_F. The highest mean mass concentration of M_F (~0.4 µg m^{-3}) observed during June and was ~3 and 2 times lower than the concentrations observed at a central European city (~1.26 µg m^{-3}) and pristine Amazonian rainforest (~0.85 µg m^{-3}), respectively. The higher difference between mean and median values of the box plots indicates the higher temporal variability. The relative difference between mean and median of N_F was found be higher than that of M_F indicating higher temporal variability of N_F during all measurement months. Averaged over the course of entire measurement period this trend was found to be consistent. The median and mean for M_F/M_T over the course of entire measurement period were 6 and 3% respectively, which is relatively low compared to previously reported studies for various other environments (Huffman et al., 2010; 2012; Artaxo and Hansson, 1995; Schumacher et al., 2013). On average the relative contribution of FBAP to TAP coarse mode particle mass was ~3 times higher (~6%) than its contribution to coarse mode particle number concentration (~2%). This is consistent with the observations that FBAPs show enhanced prevalence among the larger aerosol particles (Huffman et al., 2010).

Diurnal patterns of mass concentration

The diurnal trends in M_F for individual months and campaign average were also analyzed and are shown in Fig. 6. The corresponding diurnal trends in M_T are shown in Fig. S8. The monthly averaged diurnal trends in M_F for individual months and entire campaign exhibited similar trend corresponding to N_F. However, the prominent peak in dM_F/dlog D_a was observed at higher diameter (~3 – 4 µm), which is due to the fact that dM_F/dlog D_a has been derived from dN_F/dlog D_a assuming unit density. As observed for N_F during the month of June, the consistent morning peak was present in M_F with only difference of prominent second peak in M_F, which starts late in the evening at ~19:00 hr and further extends up to morning hours (~08:00 hr). Thereafter M_F concentration steadily decreased as the day progressed reaching minimum at around mid-day. The early morning peak in M_F concentration was consistently observed in the size range of 3 – 4 µm for the all the measurement months. The characteristic distribution of M_T (Fig. S8), however, exhibited distinct behavior as compared to both M_F and N_T. The concentration peak of <1 µm observed in N_T shifted to the higher diameter range of ~2 – 3 µm as increase in mass is more associated with presence of coarse mode particles. For example in June M_T exhibited similar diurnal feature as that of N_T. The flatter trend observed in average M_T during the month of June disappeared during the month of July and August with appearance of less prominent peak in M_T at around 12:00 hr resulting in relatively pronounced diurnal pattern (Fig. S8). The distinct diurnal patterns of M_F and M_T showed very less relative contribution of FBAP to TAP mass as

Atmos. Chem. Phys. Discuss., doi:10.5194/acp-2016-265, 2016
Manuscript under review for journal Atmos. Chem. Phys.
Published: 8 April 2016

compared to other observational sites (Huffman et al., 2010, 2012; Matthias-Maser and Jaenicke, 1995).

3.3 Size distribution of particle number and mass

Figure 7 shows the number and mass size distributions for TAPs and FBAPs averaged over the entire measurement period. The TAP number size distribution, dN_T/dlogD_a, was generally broad and dominated by a peak at the lower end of the measured size range of number size distribution (D_a≈0.9 µm; Fig. 7a). In dN_T/dlogD_a the concentrations exhibited a significant decrease above diameter ~3 µm with a long tail extending on the right hand side of the distribution. The corresponding monthly dN_T/dlogD_a are shown in Fig. S9. Overall the individual monthly dN_T/dlogD_a exhibited the similar qualitative number size distribution pattern as that of campaign averaged TAP number size distribution. Averaged over the entire measurement period, the mass size distribution, dM_T/dlogD_a (Fig. 7c), exhibited a broad peak at ~2.6 µm with an extended tail to the left side of the mass size distribution, whereas on the right side a second peak started appearing at D_a≈12 µm. The corresponding monthly averaged dM_T/dlogD_a are shown in Fig. S10. As evident from the figure the campaign average TAP mass size distribution appeared generally similar to each of the individual months. For accurate representation of mass size distribution the unit-normalized mass distribution in D_a plotted in Fig. 7 (c and d) is expected to shift to larger particle size with increased area under the curve, as D_a is directly proportional to square root of density of the particle under consideration (Huffman et al., 2010; DeCarlo et al., 2004).

The campaign average number size distribution of FBAP (Fig. 7b) exhibited monomodal shape with much narrower peak than the TAP number size distribution, with a dominant mode at D_a≈2.8 µm, which was consistent throughout measurement period. The corresponding monthly mean FBAP number size distributions are shown in Fig. S11. This peak was much prominent and narrow in the month of June with highest FBAP concentration and became less pronounced in July, with the lowest FBAP concentration. As reported by Huffman et al., (2010) multiple and broader peaks in dN_F/dlogD_a are most likely to originate from different sources and biological species. In the present study, however, we did not find multiple peaks in investigated FBAP number size distribution, suggesting that observed FBAPs comprised the particles from similar or same sources. The overall qualitative appearance of the average FBAP number size distribution is similar to that has been reported by previous measurements. For a semi-urban site in Central Europe Huffman et al., (2010) reported an average FBAP peak at 3.2 μm. Gabey et al., (2010) observed a similar peak at ~2.5 μm at a tropical rain forest site in Borneo. From a pristine Amazonian rainforest site during wet season Huffman et al., (2012) reported a similar peak at ~2.3 μm. For another pristine observational site in boreal forest in Finland Schumacher et al., (2013) reported a peak in FBAP number size distribution at ~3 μm. A similar peak at ~3 μm was also observed by Healy et al., (2014) at a rural site in Killarney national park, Ireland. This dominant peak in the range of 2 – 3 μm in FBAP number size distribution is strongly attributed to the fungal spores over the continent as reported by numerous previous researchers **(**Huffman et al., 2010, 2012; Schumacher et al., 2013, Li et al., 2011; Artaxo and Hansson, 1995; Healy et al., 2014; Gabey et al., 2010, 2013; Toprak and Schnaiter, 2013**)**. Recently Valsan et al., (2015) investigated the morphological characteristics of PBAPs from the same site during non-monsoon season and found that fungal spores constituted the major fraction of PBAPs and nominally ranged in the size range of ~3 – 10 μm, which roughly translates into equivalent aerodynamic diameter of 2 – 5 μm. The scanning electron microscopy images obtained from the filter samples occasionally collected during this field campaign showed the strong presence of variety of fungal spore in the size range of 3 – 10 μm (aerodynamic diameter 2 – 5 μm; discussed below; Fig. 17). As an overview of the comparison, the FBAP concentration values observed at Munnar are compared to the FBAP concentration ranges obtained using similar online measurements techniques from diverse environmental conditions across the globe, and the details are tabulated in Tab. 3. The campaign averaged FBAP mass size distribution is shown in Fig. 7d, which nominally appeared bimodal with very sharp primary peak at D_a≈3.2 μm and very broad but unappreciable second mode at D_a≈4 μm. The distinct presence of particle mass in the higher diameter range (>10 μm) in FBAP mass size distribution was not prominently noticed in Munnar as compared to previously reported studies (Huffman et al., 2010; 2012). In case of TAP mass size distribution the right side tail started showing positive slope at larger diameter whereas FBAP mass size distribution consistently showed the negative slope at larger diameters. Such a distinct shape of mass size distributions for TAP and FBAP reconfirms the fact that the larger particles observed in the TAP mass distribution originated from processes that did not produce particles of the biological origin as likewise reported by Huffman et al., (2010). The corresponding monthly mean FBAP mass size distributions are shown in Fig. S12. The individual month FBAP mass size distribution exhibited the similar qualitative shape to that of average campaign. As mentioned above highest FBAP mass concentration was observed in June, which coincided with a very sharp and narrow primary peak in FBAP mass size distribution, while the lowest FBAP mass concentration during July, on the other hand, coincided with a broad primary peak with lower slope.

The size-resolved ratio of FBAP to TAP averaged over the course of measurement is shown in Fig. 8 and corresponding monthly ratios are shown in Fig. S13. The relative contribution of FBAPs (dN_F) to TAPs (dN_T) in each size bin could be used to derive the relative contribution of

Atmos. Chem. Phys. Discuss., doi:10.5194/acp-2016-265, 2016
Manuscript under review for journal Atmos. Chem. Phys.
Published: 8 April 2016

biological particles to total aerosol particles at each size. As reported by Huffman et al., (2010) the assumption of unit density of each particle implies that the value of the dN_F/dN_T ratio would invariably is equal to dM_F/dM_T. The integrated N_F/N_T and M_F/M_T, however, would have the distinct values. As can be seen from Fig. 8 and S13a considerable quantitative and qualitative difference in mean (red) and median (green) curve was consistently observed in all individual months, which likely is the result of poor counting statistics and very high variability in FBAP and TAP number concentrations. Based on the results presented by Huffman et al., (2010) the mean (red) curve, best represents the N_F/N_T ratios at the upper particle sizes; hence we will stick our further discussion about N_F/N_T ratios for the present study to the mean curve. The mean N_F/N_T ratio curves for individual months and for entire campaign exhibited two dominant peaks persistently in the particle size range ~3 – 4 μm and ~6 – 8 μm. The first prominent peak in dN_F/dN_T distribution at 3 – 4 μm comprised 15 – 16% while the second peak at 6 – 8 μm represented ~14 – 15% of the FBAP material in TAP over the entire measurement period (Fig. 8). As can be observed from Fig. S13, the second peak in N_F/N_T ratios for July was higher (~12%) than the first peak (~10%) unlike other two observational months. The fact that N_F/N_T ratio is approximately zero for the particle sizes <1.7 μm indicated that FBAP mainly comprised of very small fraction of submicron aerosols at Munnar. The statistics for the individual months showed that the first peak in dN_F/dN_T was more or less consistent at ~22% during June and August except for the July when second peak in N_F/N_T ratios contributed more (~12%) than the first peak (~10%).

3.4 Focus periods

As described in Sec. 3.1 based on campaign overview the characteristics properties of FBAP and specifically TAP number concentration exhibited strong temporal variabilities, which could be

Atmos. Chem. Phys. Discuss., doi:10.5194/acp-2016-265, 2016
Manuscript under review for journal Atmos. Chem. Phys.
Published: 8 April 2016

attributed to changes in prevailing meteorological conditions especially wind direction during monsoon season at Munnar. To explore the potential impact of air mass origin on number and size distribution of FBAP and TAP, we highlight three distinct focus periods:

1. A focus period of "dusty episode" was identified when prevailing wind was predominantly Westerly/Southwesterly and air masses mainly came from the Arabian Sea. These air masses, although almost anthropogenically clean, are laden with sea salt and dust particles during the start of the monsoon, which dominate the coarse mode fraction of atmospheric aerosols (Vinoj et al., 2014; Li and Ramanathan, 2002). These dust particles observed over this region mainly originate from West Asia, North Africa, and Arabian region (Vinoj et al., 2014). During our measurement campaign, a dusty period from 14-06-2014 00:00 hr to 25-06-2014 23:55 hr was observed and is consistent with the description given above and SEM images, which showed the presence of mineral dust, obtained during dusty period (see Sec. 3.5 below). This period was marked with an accumulated rainfall of ~1015 mm, average relative humidity of 94.4±6.5%, average temperature of 17.7±1.5°C, and average wind speed 2.8±1.3 m s^{-1} (maximum wind speed of 6.7 m s^{-1}).

2. A focus period of "clean period", was observed during latter half of the monsoon season when wind direction was predominantly Westerly/Southwesterly and air masses originated over Arabian Sea. During this period, which was chosen from 09-07-2014 10:25 hr to 07-08-2014 23:55 hr, FBAP and TAP concentrations were extremely low with very weak variability. This clean period was associated with persistent rainfall (accumulated rainfall of 2650 mm), average relative humidity of 99.5±1.4%, average temperature of 16.4±0.5°C, and average wind speed 3.7±1 m s^{-1} (maximum wind speed of 8.3 m s^{-1}).

3. A focus period of "high bio" comprised three discrete events of high FBAP concentration observed from 01-06-2014 09:10 hr to 05-06-2014 18:20 hr; 26-06-2014 00:05 hr to 30-06-2014 17:00 hr; and 18-08-2014 00:00 hr to 22-08-2014 08:30 hr. Interestingly this period is marked with the very distinct metrological parameters compared to the clean period: accumulated rainfall 194 mm, average relative humidity 93.4±8.4%, average temperature 18.0±2.4°C, and average wind speed 1.2±0.8 m s^{-1} (with maximum wind speed of 4.6 m s^{-1}). Briefly, during "high bio" period stagnant air masses came from densely vegetated region located north of observational site, and relative humidity and temperature exhibited high variability.

3.4.1 Particle number and mass concentrations

The statistical distributions of N_T, N_F, M_T, and M_F for three different focus periods (dusty, clean, and high bio) are shown in Fig. 9 and tabulated in Tab. 4. Each of the focus periods discussed here did not represent equal duration of the observations. The average total particle number concentration, N_T, showed a decrease of ~70% from dusty period to clean period (~4.2 cm^{-3} and ~1.3 cm^{-3} respectively), whereas the N_T concentration during high bio period was ~1.8 cm^{-3}. The high N_T concentration during the dusty period caused the high variability between 5th and 95th percentile in N_T when averaged over entire campaign period (Fig. 3a). The fraction of dust in coarse mode aerosol, which is observed to be very high during pre-monsoon and first few days from the onset of monsoon rainfall, gradually decreased as the monsoon progressed as a result of wash out and wet deposition due to persistent rainfall in the path of air masses (Hirst 1953; Madden, 1997; Burge and Roger, 2000). The M_T exhibited similar pattern to that of N_T during three distinct focus periods with average mass concentration of ~16.3 µg m^{-3}, ~5.1µg m^{-3}, and ~7.7 µg m^{-3} for dusty, clean, and high bio periods, respectively.

Atmos. Chem. Phys. Discuss., doi:10.5194/acp-2016-265, 2016
Manuscript under review for journal Atmos. Chem. Phys.
Published: 8 April 2016

As expected, the N_F was highest during the high bio period (Fig. 9b) with an average concentration of 0.05±0.04 cm^{-3} and high variability in higher concentration range (0.06 – 0.13 cm^{-3}) as evident from the distance between 75th and 95th percentile. The N_F was found to be relatively stable during the dusty period with an average concentration of ~0.02±0.008 cm^{-3}. The average N_F concentration was found to be an order of magnitude lower during clean period (0.005±0.004 cm^{-3}) as compared to high bio period, whereas corresponding decrease in N_T from dusty to clean period (~ by factor of 3) was not of similar magnitude. We put forward following hypothesis for such a concentration difference in N_F and N_T during three distinct periods: During clean period the predominant wind direction was Westerly/Southwesterly and air masses came from Arabian Sea bringing clean marine influx marked by persistent rainfall. As a result, the coarse mode aerosol fraction (N_F and N_T) emitted locally were efficiently removed, however, the sea salt particles present in the air masses, which came from Arabian Sea contributed to TAP number concentration (see section 3.5). In addition to the efficient wet removal of FBAP due to persistent rainfall, the high RH level (average 99.5%), which causes the dew formation that further inhibit the spore release in turn reduced the FBAP concentration (Schumacher et al., 2013; Jones and Harrison, 2004). The mean values of M_F exhibited similar temporal trends and qualitative pattern as N_F, with highest mass concentration of 0.58 μg m^{-3} during high bio period, which reduced by ~86% (0.08 μg m^{-3}) during the clean period.

As anticipated the relative contribution of FBAP in TAP during dusty and clean periods was almost negligible with N_F/ N_T ratio of ~1%. Whereas during the high bio period the relative FBAP number and mass contribution to corresponding TAP was ~5% and 12% respectively.

3.4.2 Size distribution of particle number and mass concentration

Atmos. Chem. Phys. Discuss., doi:10.5194/acp-2016-265, 2016
Manuscript under review for journal Atmos. Chem. Phys.
Published: 8 April 2016

Figure 10 highlights the dN_F/dlog D_a during three distinct focus periods and corresponding dN_T/dlog D_a are shown in Fig. S14. Overall dN_F/dlog D_a exhibited pattern similar to that of campaign average.

The dN_F/dlog D_a averaged over the dusty period was dominated by a narrow peak at ~2.5 – 3.1 µm. The corresponding dN_F/dlog D_a during clean period was overall broader compared to dusty and high bio periods with gradual increase in FBAP number concentration from diameter range of ~1 - 2.3 µm, with a sharp increase thereafter, whereas downward slope exhibited the consistent pattern. dN_F/dlog D_a during high bio period exhibited relatively narrow peak at ~2.5 µm. Unlike previously reported studies (Huffman et al., 2010; 2012) the peak in dN_F/dlog D_a (D_a≈3 µm) was not reflected in dN_T/dlog D_a mostly due to relatively less contribution of FBAP in coarse mode TAP number concentration. As can be seen from Fig. S14a the total aerosol particle number size distribution, dN_T/dlog D_a, during dusty period exhibited a peak at ~0.9 µm, with a high negative slope on the left side of the distribution curve. This peak may be comprised of mineral dust and sea salt particles, as also evident from SEM images (please refer to section 3.5) and based on the previous studies investigated aerosol composition over India during monsoon season (Vinoj et al., 2014; Moorthy et al., 1991; Vinoj and Satheesh, 2003; Satheesh and Srinivasan, 2002; Li and Ramanathan, 2002). A similar peak in dN_T/dlog D_a at D_a≈0.9 µm was observed in pristine Amazonian rainforest and particles were mostly dominated by mineral dust during high dust period (Huffman et al., 2012, Fig. 5b). During clean period dN_T/dlog D_a resembled the similar shape (peaking at ~0.9 µm) to that of dusty period, however, with lower concentration. The corresponding dN_T/dlog D_a distribution (Fig. S14c), during high bio period, exhibited multiple peaks and appeared noisy for D_a<1 µm with increasing trend in TAP number concentration for the lower diameter range of the distribution. The downward slope for D_a>1 µm exhibited consistent shape (mean curve) compared to distributions observed during other two focus periods.

The FBAP mass size distribution (Fig. 11) during dusty period was dominated by bimodal peaks with prominent peak at ~3 μm and relatively less pronounced peak in the range of ~4 – 6 μm showing broader tail on the right side of the distribution curve. The dM_F/dlog D_a, during clean period, exhibited similar bimodal peaks with extended shoulder in the diameter range from ~4 to 7 μm. The dM_F/dlog D_a distribution during high bio period was distinct compared to two other focus periods discussed above with a prominent monomodal peak at ~3 μm. The primary peak observed in dM_F/dlog D_a in the range of ~3 to 4 μm was consistent during individual months and different focus periods. TAP mass size distribution (Fig. S15) exhibited similar qualitative pattern to that of campaign averaged dM_T/dlog D_a with peak between ~2.5 to 3.5 μm with an extended tail on the right side, which gradually increased for D_a>13 μm.

The size resolved ratio of FBAP to TAP particles averaged for three distinct focus periods is shown in Fig. 12. As evident from the figure the largest fraction of FBAP particles during dusty period occurred between ~ 6 – 9 μm (~20%) with relatively small contribution in the size range of ~ 3 – 4 μm (~7%). The dN_F/dN_T exhibited the sloping tails on both the sides of the distribution with steep slope on the right side. The fact that N_F/N_T is approximately zero for the particle size range below ~1.5 μm is consistent with previous observations reported from semi urban site in central Europe and during wet season of pristine Amazonian rainforest (Huffman et al., 2010; 2012). During the clean period the maximum contribution of FBAP to TAP number concentration reduced to ~10.5% in the diameter range of ~ 6 to 9 μm with another prominent, but relatively smaller contributing peak, at ~3 – 4 μm with relative contribution of ~8%. During high bio period the maximum contribution of FBAP to TAP occurred between size range of ~ 3

Atmos. Chem. Phys. Discuss., doi:10.5194/acp-2016-265, 2016
Manuscript under review for journal Atmos. Chem. Phys.
Published: 8 April 2016

– 8 µm with contribution range of ~28 – 19% and relatively broad dN_F/dN_T distribution. Interestingly during high bio period the highest contribution of FBAP to TAP number concentration occurred at D_a≈3.5 µm, as opposed to other two focus periods when highest contribution was observed in the larger diameter ranges of ~ 6 – 8 µm. N_F/N_T was consistently found to be equal to zero for the diameter beyond 13 µm indicating that FBAP comprised extremely small fraction of total aerosol particles (Huffman et al., 2010; 2012). The two prominent peaks observed during focus periods were clearly evident in campaign-averaged dN_F/dN_T (Fig. 8; peaks at ~3.5 and 6 µm).

3.4.3 Diurnal patterns

A prominent early morning peak in N_F during high bio period in the diameter range of 1.5 – 3 µm was observed from 06:00 hr to 08:00 hr, which clearly reflected in campaign averaged diurnal patterns at the same hour of the day. The diurnal variations in N_F during dusty and clean periods were not so pronounced (Fig. 13) as compared to the variations during high bio period. During dusty period N_F showed slightly high concentration starting from ~20:00 hrs and persistently remained high until early morning without any variations, whereas during clean period N_F concentration consistently remained flat throughout 24 hrs. The evening peak observed during dusty period, however, was clearly absent during high bio period. A moderately pronounced peak in N_F during evening hours at ~20:00 hr during dusty periods might indicate that releasing mechanism of bioaerosols was efficient as a result of nocturnal sporulation. This can further imply that the morning and late evening peaks in $dN_F/d\log D_a$ at D_a≈3 µm most likely resulted from different type of spores (Hirst, 1953). As listed by Huffman et al., (2012) the emission and dispersal of bioaerosols is strongly coupled with environmental variables such as solar radiation, temperature, and relative humidity and each of these variables have strong

Atmos. Chem. Phys. Discuss., doi:10.5194/acp-2016-265, 2016
Manuscript under review for journal Atmos. Chem. Phys.
Published: 8 April 2016

diurnal cycles. It has been well documented that relative humidity, in particular, plays an important role in active wet discharge of fungal spores (Adhikari et al., 2006; Burch and Levetin, 2002; Elbert et al., 2007; Jones and Harrison, 2004; Quintero et al., 2010; Zhang et al., 2010) , which constitutes major fraction of atmospheric bioaerosols (Ansari et al., 2015; Bauer et al., 2008; Bowers et al., 2013; Fröhlich-Nowoisky et al., 2009; Sesartic and Dallafior, 2011; Spracklen and Heald, 2014). The meteorological parameters exhibited pronounced diurnal variations during high bio period, where RH decreased to a level (~60 – 80%), which is considered to be favorable for release of the fungal spores (Jones and Harrison, 2004; Santarpia et al., 2013). During dusty and clean period the persistence of high RH values in the range of ~90 – 100%, however, might have inhibited the active wet discharge of fungal spore (Schumacher et al., 2013;) thus resulting the weak diurnal variation in N_F. Unlike N_F, N_T remained flat without any pronounced diurnal variations during three distinct focus periods (Fig. S16). The corresponding diurnal cycle of FBAP mass concentration and size distributions for three focus periods are shown in Fig. S17. M_F exhibited similar diurnal patterns to that of N_F during three focus periods. M_T as like N_T remained flat during dusty period, however exhibited slightly pronounced diurnal pattern during clean and high bio period between 09:00 hrs and 16:00 hrs (Fig. S18).

3.5 SEM images

Figure 14 shows the exemplary SEM images of biological particle types often observed during the SW monsoon season at Munnar. The details about the sampling techniques, instrument used, etc. for obtaining these bioaerosol images are discussed in details by Valsan et al., (2015). Note that these images are not being presented here for any quantitative purpose and to draw any specific scientific conclusions but mainly to showcase the particle types consistently observed throughout the measurement period. As seen from the SEM images majority of the particles are mostly likely fungal spores. Based on their distinct morphology the spores in Fig. 14a-c most likely appeared to be of Basidiospores. The appearance of small protuberances on the surface suggests that the spore in Fig. 14a most likely belonged to the *Hydnaceae* family (Grand and Vandyke, 1976; Valsan et al., 2015). The Basidiospores shown in Fig. 14b and c were seen in abundance in all the samples collected during the campaign. Some of the spores observed appeared to be coated with salt particles (Fig 14e) and might have been carried from a distant source by the SW monsoon winds. The spores shown in Fig 14 (d and f) most likely appeared to be spores of Ascomycota division. The particle shown in Fig. 14g was most likely a mineral dust particle sampled during high dusty episode. Similar particles of varying size during dusty episode were consistently observed during SEM analysis. Fig 14h and i shows the images of the typical sea salt particles observed during samples collected at Munnar during measurement campaign when wind predominantly came from Westerly/Southwesterly direction travelling over Indian Ocean and Arabian Sea.

3.6 Meteorological Correlations

The results obtained with UV-APS data analysis during the campaign at Munnar were plotted with respect to meteorological parameters to investigate factors responsible for bioaerosol release and their variations in the atmosphere.

Impact of wind direction

The wind rose diagrams scaled by N_{F}, D_{g}, and $D_{\mathrm{g,T}}$ were also prepared for entire measurement period and three distinct focus periods. These plots are in a way similar to the traditional wind rose diagram (Fig. S19) except, instead of wind speed, they are scaled by characteristic FBAP and TAP parameters, which indicate the frequency of occurrence of respective parameter with respect to wind direction (Sherman et al., 2015). As can be seen from Fig. S19, predominant wind direction during entire campaign was Westerly/Southwesterly with frequency of occurrence of about ~90%. The wind speed broadly ranged between 2 – 5 m s^{-1} with no prominent diurnal variations. The overall wind direction and back trajectory analysis (Fig. 1) shows that the sampled air masses may have had their origin over the Indian Ocean thereafter turning eastward after crossing the equator and travelling several hundred kilometers over Arabian Sea before reaching the observational site (Fig. 1). The predominant wind pattern during dusty (>95% frequency of occurrence; 2 – 6 m s^{-1}) and clean periods (~100 frequency of occurrence; 2 – 6 m s^{-1}) was Westerly/Southwesterly. Whereas during high bio period only ~50% of the time winds came from Westerly/Southwesterly direction and rest comprised the stagnant and calm (0 – 2 m s^{-1}) winds from all other directions with highest contribution of northerly winds (Fig. S19). .

Wind rose diagram scaled by FBAP number concentration is shown in Fig. 15. During the entire campaign the predominant wind showed that ~85% of the time FBAP concentration occurred in the range of 0 – 0.05 cm^{-3} (Fig. 15a) occasionally exceeding 0.05 cm^{-3} and was contributed by Westerly/Southwesterly winds. The occurrence of relatively low FBAP concentration during entire campaign is consistent with low concentration occurrence during dusty (0 – 0.05 cm^{3}; >90% frequency of occurrence) and clean (<0.01 cm^{3}; ~90% frequency of occurrence) periods. During high bio period the FBAP concentration, >0.05 cm^{3} exhibited ~40% frequency of occurrence of which ~50% was contributed by predominant wind from North and Northwest.

Similarly the wind rose diagram scaled by geometric mean diameter (D_g) of $dN_F/d\log D_a$, is shown in Fig. 16. The average size of the FBAP particles associated with Westerly/Southwesterly winds when analyzed for entire the campaign ranged between 2 – 4 μm of which ~65% of the time D_g was observed to be ≤3 μm. During three distinct focus periods the frequency of occurrence of FBAP particles in the higher size range (3 – 4 μm) was strongly associated with the Westerly/Southwesterly winds (Figs. 16b – d). The corresponding wind rose diagram scaled by geometric mean diameter of dN_T/dlog D_a ($D_{g,T}$) is shown in Fig. S20. During entire measurement campaign the frequency of occurrence of $D_{g,T}$ in the size range of 0.8 – 0.9 μm was ~70% and was mostly associated with Westerly/Southwesterly winds. During dusty period particles in the size range of 0.8 – 0.9 μm diameter contributed for >95% frequency of occurrence for the entire size range, whereas during clean period ~20% occurrence of the particles in the size range other than 0.8 – 0.9 μm were also observed. On the other hand during high bio period total particles in the size range 0.5 – 0.8 μm were observed with ~50% frequency of occurrence constituted by varying wind patterns mostly dominated by northerly winds.

The FBAP concentration exhibited strong dependence on the wind direction for this observational site. During the high bio period the increase in frequency of occurrence of FBAP number concentrations >0.1 cm^{-3} coincided with stagnant wind coming from North and Northwest (Fig. 17a). During high bio period, as like dusty and clean periods the predominant wind pattern was Westerly/Southwesterly, however, with relatively low frequency of occurrence as compared to other two periods. To have the better understanding of relative contribution of wind direction in high FBAP number concentration during high bio period, we prepared the separate wind rose diagrams for FBAP concentration >0.1 cm^{-3} and <0.1 cm^{-3} as shown in Fig. 17. The FBAP number concentration >0.1 cm^{-3} was associated with calm (0 – 1 m s^{-1}; ~80% frequency of occurrence) and predominant Northerly winds (Fig. 17a) as opposed to high wind speed (2 – 5 m s^{-1}) and predominant Westerly/Southwesterly winds for the FBAP number concentration <0.1 cm^{-3} (Fig. 17b). The calm northerly winds coming over from densely

Atmos. Chem. Phys. Discuss., doi:10.5194/acp-2016-265, 2016
Manuscript under review for journal Atmos. Chem. Phys.
Published: 8 April 2016

Atmospheric Chemistry and Physics Discussions

vegetated regions in combination with local FBAP sources during high bio period could be the strong reason for the built up resulting in higher FBAP number concentration during this episode, whereas, Westerly/Southwesterly winds were consistently marked by very low FBAP number concentration mostly owing to higher wind speeds. Further, it might also due to the fact that the air masses arriving at observational site originated over cleaner marine region, which may be potential but weak source of bioaerosols combined with possible wash out/wet deposition due to persistent rainfall during the transport. Nominally the frequency of occurrence of larger particles (3 – 4 μm) during Westerly/Southwesterly winds was high compared to the Northerly winds, where particles were mostly of smaller size (1 – 3 μm). We hypothesize that during Northerly wind the bioaerosols were mostly comprised of Basidiospores, which is consistent with SEM images obtained during measurement period. Frohlich-Nowoisky et al., (2012) reported that, region with dominant prevalence of marine air masses have larger proportions of Ascospores and in contrast, the continental air masses exhibit higher proportions of Basidiospppres. However, due to technical difficulties associated with sampling we could not establish the fact that spores observed at this observational site during Westerly/Southwesterly winds were dominated by Ascospores and these details will be addressed in follow up studies. The corresponding wind rose scaled by $D_{g,T}$ obtained from dN_T/dlog D_a is shown in Fig. S21.

As shown in Tab. 5 the wind speed was observed to be negatively affecting the N_F during entire measurement period and is consistent with previously reported studies (Hameed et al., 2012; Almaguer et al., 2013; Lyon et al., 1984; Quintero et al., 2010). The increased N_F concentration levels during calm and stagnant wind might indicate that observed bioaerosols were dominated by the local source rather than transported from longer distances (Sadys et al., 2014; Hara and Zhang, 2012; Bovallius et al., 1978; Maki et al., 2013; Prospero et al., 2005; Creamean et al.,

Atmos. Chem. Phys. Discuss., doi:10.5194/acp-2016-265, 2016
Manuscript under review for journal Atmos. Chem. Phys.
Published: 8 April 2016

2013) as lower wind speed may actually increase emission of some specific type of spores (Huffman et al., 2012; Jones and Harrison, 2004; Troutt and Levetin, 2001; Kurkela, 1997).

3.6.1 Correlation with relative humidity and temperature

Correlation coefficient derived between N_F and relative humidity averaged over the entire campaign is shown in Fig. 18 and corresponding R^2 values for three distinct focus periods are shown in Tab. 5. In general an increase in N_F concentration with increasing relative humidity was observed with moderate correlation coefficient (R^2=0.58). Depending upon the type of bioaerosols, geographical location, and local climate, N_F has shown varied dependence on relative humidity and precise response of the spore concentration to relative humidity is difficult to characterize. For example number of studies have shown that spores of genus like *Cladosporium*, *Alternaria*, and *Epiccocum* are known to exhibit the negative correlation with relative humidity (Oliveira et al., 2010; Herrero et al., 1996; Kurkela, 1997; Oh et al., 1998; Healy et al., 2014) on the other hand studies have also found these spores to be positively correlated with relative humidity (Quintero et al., 2010; Hjelmroos, 1993; Ho et al., 2005). Whereas genus like *Ustilago* and some other Basidiospores may as well exhibit strong positive correlation with relative humidity (Sabariego et al., 2000; Quintero et al., 2010; Ho et al., 2005; Calderon et al., 1995). Further, Ascospores concentrations are known to increase during and after rainfall (Burch and Levetin, 2002; Elbert et al., 2007; Hasnain, 1993; Hirst, 1953; Toutt and Levetin, 2001; Lyon et al., 1984; Oh et al., 1998) whereas Basidiospores exhibited a strong resemblance to the diurnal pattern of relative humidity (Li and Kendrick 1994; Hasnain 1993; Tarlo et al., 1979; Trout and Levetin 2001). Almaguer et al., (2013) have reported that in tropical region relative humidity has greater influence than temperature on the airborne spore counts and may be a pre-requisite for release of spores (Hollins et al., 2004). Thus, the combination of persistent threshold relative humidity (~60 – 95% as reported by Ho et al., 2005) and rainfall can cause the increase in the spore concentration and the excessive and persistent rain, however, tends to wash the spore out of the atmosphere further reducing their concentration levels (Burge 1986; Horner et al., 1992; Troutt and Levetin, 2001). Based on these arguments combined with observed meteorological conditions we expect that the bioaerosols reported here from Munnar mainly consisted of Basidiospores during the SW monsoon season as also evident from SEM images (discussed above). This is consistent with results reported by Valsan et al., (2015) where they found the dominant presence of dry air spora (*Cladosporium*) during relatively dry and warm weather from the same observational site. In general, N_F and N_F/N_T decreased with increasing wind speed (R^2=0.6 and R^2=0.78, respectively) indicating that wind speed may be one of the strong factors for observed high N_F concentrations at this site. As compared to previously reported correlation between N_F and meteorological parameters (Santarpia et al., 2013), the relations shown for this observational site appeared to be more robust and conclusive. For example since the variability derived in N_T (N_T - $N_{T,min}$/ $N_{T,max}$- $N_{T,min}$; not shown here) was more consistent and high as compared to variability derived in N_F (N_F – $N_{F,min}$/ $N_{F,max}$- $N_{F,min}$), which was more episodic and hence one would expect the weak correlation between N_T and meteorological parameters (Tab. 5).

On the other hand several studies have reported that in temperate regions temperature is probably the most important meteorological parameter affecting the spore concentration (Levetin and Horner, 2002; Adhikari et al., 2006) with highest spore concentration during summer season (Emberlin et al., 1995; Hasnain, 1993; Herrero et al., 1996; Hjelmroos, 1993; Li et al., 2011; Schumacher et al., 2013). When the relation between temperature and spore concentration was investigated on averaged diurnal basis, however, spore concentration have been observed to decrease with the increasing temperature (Burch and Levetin, 2002; Calderon et al., 1995; Sabariego et al., 2000; Schumacher et al., 2013; Trejo et al., 2013). Consistent with this trend, we have found significant negative correlation between N_F and temperature (R^2=0.65) averaged over the entire measurement period at Munnar. The correlation coefficient between N_F and temperature for three distinct focus periods is given in Tab. 5. The correlation coefficient between N_F/N_T and meteorological parameters in general yielded higher R^2 values. Note, however, that the interpretation presented here based on the correlation analyses performed between N_F and meteorological parameters were intended not to generalize and extrapolate conclusions to various other ecosystems (including Indian region) and different seasons of the year (including non-monsoon in India) but were presented to take an opportunity to formulate preliminary hypothesis about role of meteorological parameters in governing the variaibilites of bioaerosls specific to this observational site for the monsoon season only.

4 Summary and Conclusions

During these maiden online measurements of biological aerosol particles we operated a UV-APS continuously during the SW monsoon season (1.June – 21.August) of 2014 at a high-altitude site of Munnar in Western Ghats in Southern tropical India. The number and mass size distributions and corresponding concentrations of biological aerosol were quantified for three distinct focus periods namely dusty period, high-bio period, and clean period identified based on the prominent wind direction. We have analyzed the three month time series of integrated coarse particle number and mass concentrations, as well as particle number and mass size distributions of both, the total and fluorescence biological aerosol particles. Over the course of entire measurement period the coarse particle number concentration of FBAPs varied in the range of 0.2×10^{-3} cm^{-3} to 0.63 cm^{-3} with an arithmetic mean value of 0.02 cm^{-3} (±0.02 cm^{-3}). This average concentration accounted for 0.04 – 53% (mean value 2.1%±4.05%) of the total coarse particle number concentration. The coarse particle mass concentrations of FBAPs varied in the range of 0.5×10^{-3} – 4.93 µg m^{-3} with an arithmetic mean (±standard deviation) value of 0.24 (±0.28) µg m^{-3}.

The average FBAP concentration during the entire measurement period was found to be highest in June (0.03 cm^{-3}) and lowest in July (0.007 cm^{-3}). The FBAP concentrations observed at Munnar during SW monsoon season are within the range but slightly on the lower side of the bioaerosol concentrations reported by previous researchers using various online and offline techniques. Numerous other studies from different part of the world have reported detailed description about observed biological aerosol particle number concentrations using offline and online techniques from various environments (Despres et al., 2007; Huffman et al., 2010, 2012; Adhikari et al., 2004; Bovallius et al., 1978; Bowers, et al., 2009, 2013; Lee et al., 2010; Matthias-Maser and Jaenicke, 1995; Matthias-Maser et al., 2000; Shaffer and Lighthart, 1997; Tong and Lighthart, 1999; Wang et al., 2007; Li et al., 2011; Hameed et al., 2009; Bauer et al., 2008; Schumacher et al., 2013; Gabey et al., 2010, 2011, 2013; Saari et al., 2015; Toprak and Schnaiter, 2013; Healy et al., 2014). For brevity, here we compare the number concentrations observed at Munnar only with number concentrations from varying environments reported by previous researchers using online measurements. Huffman et al., (2010) have reported coarse mode average FBAP number concentration from four months of measurement to be 0.03 cm^{-3}, which constituted ~4% of total coarse mode particles from a semi-urban site of Mainz in Central Europe. The median FBAP concentration during the wet season of pristine tropical Amazonian rainforest region was found be 0.07 cm^{-3}, which constituted ~24% of total coarse mode particle number concentration (Huffman et al., 2012). By analyzing the full one-year observations from Boreal forest in Hyytiala and pine forest in Colorado, Schumacher et al., (2013) reported highest

Atmos. Chem. Phys. Discuss., doi:10.5194/acp-2016-265, 2016
Manuscript under review for journal Atmos. Chem. Phys.
Published: 8 April 2016

FBAP concentration in summer of 0.046 cm^{-3} (constituting ~13% of total coarse mode particles) and 0.03 cm^{-3} (constituting ~8.8% of total coarse mode particles), respectively. Healy et al., (2014) reported the average FBAP concentration of ~0.01 cm^{3} using the UV-APS measurements carried out with in the Killarney national park, Kerry situated in Southwest of Ireland. Gabey et al., (2013) by performing the measurements at a high altitude cite in central France reported averaged FBAP concentration of 0.012 cm^{-3} and 0.095 cm^{-3} using two-wavelength (280 nm and 370 nm respectively) single-particle UV-induced fluorescence spectrometer. Gabey et al., (2010) from tropical rainforest in Borneo, Malaysia reported that mean FBAP number fraction in the size range of 0.8 – 20 µm was ~55% and ~28% below and above the forest canopy, respectively. It is important to note, however, that the measurement results compared here were obtained from different instrumentation operating with different wavelength. Nevertheless, the FBAP number concentrations observed under various environmental conditions are largely comparable to the FBAP number concentration observed at Munnar during SW monsoon season. Note that the relative contribution of FBAP number concentration to total coarse mode particles may show a strong spatial variability.

The average observed $dN_F/d\log D_a$ exhibited a peak at ~3 µm, which was consistent even during distinct focus periods with slight quantitative variation in the FBAP number concentration. Such a consistency in the peak of $dN_F/d\log D_a$ during entire measurement period is an indication of the fact that sources and type of bioaerosols did not exhibit considerable variability and diversity at Munnar during SW monsoon season. The peak observed in $dN_F/d\log D_a$ in this study is consistent with range of the peaks published by previous researchers. At a semi-urban site in Central Europe the peak in $dN_F/d\log D_a$ was observed at ~3 µm (Huffman et al., 2010). In pristine tropical rainforest region of Amazonia a peak in $dN_F/d\log D_a$ was found at ~2.5 µm

(Huffman et al., 2012). Whereas the peak in dN_F/dlog D_a at a boreal forest in Finland exhibited a strong seasonal dependence with different modes at ~1.5 µm, ~3 µm, and ~5 µm indicating differences in the bioaerosol sources (Schumacher et al., 2013). In the pine forest of Colorado the distinct peaks were observed at ~1.5 µm and ~5 µm (Schumacher et al., 2013). The mode at ~3 µm is likely due to the fungal spore whose release mechanism is strongly governed by the combination of relative humidity and temperature (Huffman et al., 2010 and references therein).

On the diurnal scale a pronounced diurnal cycle with ~3 µm peak with a maximum concentration at ~06:00 hr was observed when averaged over entire measurement period. This general pattern is consistent with previous studies reporting the early morning peak in FBAP concentration for various environmental conditions (Healy et al., 2014; Huffman et al., 2012; Schumacher et al., 2013; Toprak and Schnaiter, 2013). The early morning peak, which in the present case appears to be strongly governed by the diurnal variations in relative humidity, is most likely to be contributed by Basidiospores as their release in the atmosphere is strongly coupled with relative humidity (Adhikari et al., 2006; Burch and Levetin, 2002; Hasnain, 1993; Healy et al., 2014; Ho et al., 2005; Huffman et al., 2012). This is also consistent with the SEM images shown and discussed above.

The meteorological parameters were observed to correlate significantly with FBAP concentration at Munnar. When investigated on a daily averaged basis (24 hr), however, no significant correlation between N_F and meteorological parameters except moderate negative correlation with precipitation was observed. During the entire measurement campaign, except on few occasions no significant variations in temperature and relative humidity was observed. This in combination with persistent rainfall resulting in the wash out/wet deposition of biological aerosol particles might have caused such a weak correlation for a daily averaged (24 hr) analysis. On a diurnal scale, however, a significant correlation between N_F and meteorological parameters was observed. We observed that N_F followed the similar diurnal trend to that of relative humidity and was anti-correlated with temperature. As reported by previous studies from selected locations (Huffman et al., 2013; Schumacher et al., 2013; Prenni et al., 2013; Hirst 1953) we did not observe any sharp increase in N_F concentration immediately after or during rainfall. We hypothesize that the spore built-up and release of certain species can happen only at certain threshold relative humidity (Jones and Harrison, 2004). Under the dry environmental conditions where relative humidity levels rarely attain such threshold required for fungal spore release can cause the strong built up of fungal spores inside fungal bodies. Under these conditions precipitation can cause the relative humidity levels to increase up to threshold required for fungal spore release in combination with mechanical splashing due to raindrops, and can cause the sudden and sharp increase in spore concentrations. On the contrary, like in present case, the incessant persistence of high humidity conditions can cause the continuous release of the spore without an opportunity for built-up of fungal spores in fungal body to be released during rainfall. It is also reported that persistent high levels of relative humidity can inhibit the sporulation (Schumacher et al., 2013) further considerably reducing the spore release. The correlation between N_F and wind speed was found to be strongly negative. Since majority of the spore release was dominated by the local sources, the stong winds coming over from West/Southwest direction, which were relatively clean, might have caused the dilution of air mass thus reducing the spore concentration.

Overall, the long-term measurements reported in this manuscript showed the quantitative and qualitative agreement with previously reported studies. The emissions and abundance of biological aerosol particles in Western Ghats air during monsoon season appeared to be closely linked to the variaiblities in the meteorological parameters. As reported by Huffman et al., (2012) and corroborated by the observations reported in this study, UV-APS is successfully able to detect the aerosol particles of biological origin, however, may pose certain limitations in scientific interpretation from the obtained data. The scatter plot analysis carried out between N_F and N_T for submicron and supermicron particles indicated that submicron particles at this observational site were also dominated by aerosol particles of biological origin, thus indicating the lowest possible interference from particles of anthropogenic origin known to exhibit the fluorescence at the prescribed wavelength used in UV-APS. Hence, given observational site can be termed as relatively pristine while under the influence of SW monsoon season. The contrasting characteristics of this observational site associated with pollution and interference of non-biological aerosol particles in fluorescence will be discussed in follow up studies. We propose and intend to take forward these studies by means of performing simultaneous online measurements of biological aerosol particle number concentrations in high time and size resolution under contrasting environments during distinct meteorological seasons over Indian region. This future work could be supplemented with advanced offline measurement techniques including SEM analysis, DNA analysis, and fluorescence microscopy of the samples collected in parallel with the measurements. We believe that such a comprehensive approach over Indian region would be helpful in understanding the possible tight coupling between aerosol and hydrological cycle especially during monsoon. This could also help to better understand the implication of biological aerosols on crops and human health where agricultural industry has the major share in GDP to cater the need of 18% of the world's total population.

Acknowledgement:

Atmos. Chem. Phys. Discuss., doi:10.5194/acp-2016-265, 2016
Manuscript under review for journal Atmos. Chem. Phys.
Published: 8 April 2016

SSG acknowledge the combined financial support from Max Planck Society and Department of Science and Technology, Government of India under the Max Planck Partner Group Program. Authors are thankful to Akila M, Hema P, Shika S, Aleena, Hasitha, Reshma, Sanu, and Tabish U. Ansari for their support in planning, execution, and completion of the measurement campaign. Authors thankfully acknowledge the support from Gerhard Lammel, Multiphase Chemistry Department, Max Planck Institute for Chemistry for his support during campaign and providing the meteorological data for comparison. Authors are grateful to the Sophisticated Analytical Instrument Facility (SAIF), IIT Madras for making SEM available for morphological analysis. Authors gratefully acknowledge US Geological Survey for the topography data in DEM format and NOAA ARL for providing HYSPLIT air mass back trajectory calculations.

References:

Adhikari, A., Sen, M. M., Gupta-Bhattacharya, S., and Chanda, S.: Air-borne viable, non-viable, and allergenic fungi in a rural agricultural area of India: a 2-year study at five outdoor sampling stations, Science of the Total Environment, 326, 123-141, 10.1016/j.scitotenv.2003.12.007, 2004.

Adhikari, A., Reponen, T., Grinshpun, S. A., Martuzevicius, D., and LeMasters, G.: Correlation of ambient inhalable bioaerosols with particulate matter and ozone: A two-year study, Environmental Pollution, 140, 16-28, 10.1016/j.envpol.2005.07.004, 2006.

Agranovski, V., Ristovski, Z., Hargreaves, M., Blackall, P. J., and Morawska, L.: Performance evaluation of the UVAPS: influence of physiological age of airborne bacteria and bacterial stress, Journal of Aerosol Science, 34, 1711-1727, 10.1016/s0021-8502(03)00191-5, 2003.

Agranovski, V., Ristovski, Z. D., Ayoko, G. A., and Morawska, L.: Performance evaluation of the UVAPS in measuring biological aerosols: Fluorescence spectra from NAD(P)H coenzymes and riboflavin, Aerosol Sci. Technol., 38, 354-364, 10.1080/02786820490437505, 2004.

Agranovski, V., and Ristovski, Z. D.: Real-time monitoring of viable bioaerosols: capability of the UVAPS to predict the amount of individual microorganisms in aerosol particles, Journal of Aerosol Science, 36, 665-676, 10.1016/j.jaerosci.2004.12.005, 2005.

Almaguer, M., Aira, M.-J., Rodríguez-Rajo, F. J., and Rojas, T. I.: Temporal dynamics of airborne fungi in Havana (Cuba) during dry and rainy seasons: influence of meteorological parameters, International Journal of Biometeorology, 58, 1459-1470, 10.1007/s00484-013-0748-6, 2013.

Andreae, M. O., and Rosenfeld, D.: Aerosol-cloud-precipitation interactions. Part 1. The nature and sources of cloud-active aerosols, Earth Science Reviews, 89, 13-41, 2008.

Ansari, T. U., Valsan, A. E., Ojha, N., Ravikrishna, R., Narasimhan, B., and Gunthe, S. S.: Model simulations of fungal spore distribution over the Indian region, Atmospheric Environment, 122, 552-560, http://dx.doi.org/10.1016/j.atmosenv.2015.10.020, 2015.

Artaxo, P., and Hansson, H. C.: Size distribution of biogenic aerosol-particles from the Amazon basin, Atmospheric Environment, 29, 393-402, 10.1016/1352-2310(94)00178-n, 1995.

Bauer, H., Schueller, E., Weinke, G., Berger, A., Hitzenberger, R., Marr, I. L., and Puxbaum, H.: Significant contributions of fungal spores to the organic carbon and to the aerosol mass balance of the urban atmospheric aerosol, Atmospheric Environment, 42, 5542-5549, 10.1016/j.atmosenv.2008.03.019, 2008.

Bhati, H. S., and Gaur, R. D.: Studies on Aerobiology - Atmospheric fungal spores, New Phytologist, 82, 519-527, 10.1111/j.1469-8137.1979.tb02678.x, 1979.

Bovallius, A., Bucht, B., Roffey, R., and Anas, P.: 3-Year investigation of natural airborne bacterial-flora at 4 localities in Sweden, Applied and Environmental Microbiology, 35, 847-852, 1978.

Bowers, R. M., Lauber, C. L., Wiedinmyer, C., Hamady, M., Hallar, A. G., Fall, R., Knight, R., and Fierer, N.: Characterization of Airborne Microbial Communities at a High-Elevation Site and Their Potential To Act as Atmospheric Ice Nuclei, Applied and Environmental Microbiology, 75, 5121-5130, 10.1128/aem.00447-09, 2009.

Bowers, R. M., Clements, N., Emerson, J. B., Wiedinmyer, C., Hannigan, M. P., and Fierer, N.: Seasonal Variability in Bacterial and Fungal Diversity of the Near-Surface Atmosphere, Environmental Science & Technology, 47, 12097-12106, 10.1021/es402970s, 2013.

Brosseau, L. M., Vesley, D., Rice, N., Goodell, K., Nellis, M., and Hairston, P.: Differences in detected fluorescence among several bacterial species measured with a direct-reading particle sizer and fluorescence detector, Aerosol Sci. Technol., 32, 545-558, 10.1080/027868200303461, 2000.

Burch, M., and Levetin, E.: Effects of meteorological conditions on spore plumes, International Journal of Biometeorology, 46, 107-117, 10.1007/s00484-002-0127-1, 2002.

Burge, H. A.: Some comments on the aerobiology of fungus spores, Grana, 25, 143-146, 1986.

Burge, H. A., and Rogers, C. A.: Outdoor allergens, Environmental Health Perspectives, 108, 653-659, 10.2307/3454401, 2000.

Burrows, S. M., Butler, T., Jöckel, P., Tost, H., Kerkweg, A., Pöschl, U., and Lawrence, M. G.: Bacteria in the global atmosphere - Part 2: Modeling of emissions and transport between different ecosystems, Atmos. Chem. Phys., 9, 9281-9297, 2009.

Calderon, C., Lacey, J., McCartney, H. A., and Rosas, I.: Seasonal and diurnal-variation of airborne basidiomycete spore concentrations in Mexico-city, Grana, 34, 260-268, 1995.

Chakraborty, P., Gupta-Bhattacharya, S., Chakraborty, C., Lacey, J., and Chanda, S.: Airborne allergenic pollen grains on a farm in West Bengal, India, Grana, 37, 53-57, 1998.

Coz, E., Artinano, B., Clark, L. M., Hernandez, M., Robinson, A. L., Casuccio, G. S., Lersch, T. L., and Pandis, S. N.: Characterization of fine primary biogenic organic aerosol in an urban area in the northeastern United States, Atmospheric Environment, 44, 3952-3962, 10.1016/j.atmosenv.2010.07.007, 2010.

Atmos. Chem. Phys. Discuss., doi:10.5194/acp-2016-265, 2016
Manuscript under review for journal Atmos. Chem. Phys.
Published: 8 April 2016

Creamean, J. M., Suski, K. J., Rosenfeld, D., Cazorla, A., DeMott, P. J., Sullivan, R. C., White, A. B., Ralph, F. M., Minnis, P., Comstock, J. M., Tomlinson, J. M., and Prather, K. A.: Dust and Biological Aerosols from the Sahara and Asia Influence Precipitation in the Western U.S, Science, 339, 1572-1578, 10.1126/science.1227279, 2013.

DeCarlo, P. F., Slowik, J. G., Worsnop, D. R., Davidovits, P., and Jimenez, J. L.: Particle morphology and density characterization by combined mobility and aerodynamic diameter measurements. Part 1: Theory, Aerosol Sci. Technol., 38, 1185-1205, 2004.

DeLeon-Rodriguez, N., Lathem, T. L., Rodriguez-R, L. M., Barazesh, J. M., Anderson, B. E., Beyersdorf, A. J., Ziemba, L. D., Bergin, M., Nenes, A., and Konstantinidis, K. T.: Microbiome of the upper troposphere: Species composition and prevalence, effects of tropical storms, and atmospheric implications, Proceedings of the National Academy of Sciences of the United States of America, 110, 2575-2580, 10.1073/pnas.1212089110, 2013.

Despres, V. R., Nowoisky, J. F., Klose, M., Conrad, R., Andreae, M. O., and Poschl, U.: Characterization of primary biogenic aerosol particles in urban, rural, and high-alpine air by DNA sequence and restriction fragment analysis of ribosomal RNA genes, Biogeosciences, 4, 1127-1141, 2007.

Despres, V. R., Huffman, J. A., Burrows, S. M., Hoose, C., Safatov, A. S., Buryak, G., Frohlich-Nowoisky, J., Elbert, W., Andreae, M. O., Poschl, U., and Jaenicke, R.: Primary biological aerosol particles in the atmosphere: a review, Tellus Series B-Chemical and Physical Meteorology, 64, 10.3402/tellusb.v64i0.15598, 2012.

Du, C., Liu, S., Yu, X., Li, X., Chen, C., Peng, Y., Dong, Y., Dong, Z., and Wang, F.: Urban Boundary Layer Height Characteristics and Relationship with Particulate Matter Mass Concentrations in Xi'an, Central China, Aerosol and Air Quality Research, 13, 1598-1607, 10.4209/aaqr.2012.10.0274, 2013.

Elbert, W., Taylor, P. E., Andreae, M. O., and Poeschl, U.: Contribution of fungi to primary biogenic aerosols in the atmosphere: wet and dry discharged spores, carbohydrates, and inorganic ions, Atmospheric Chemistry and Physics, 7, 4569-4588, 2007.

Emberlin, J., Newman, T., and Bryant, R.: The incidence of fungal spores in the ambient air and inside homes: Evidence from London, Aerobiologia, 11, 253-258, 10.1007/bf02447205, 1995

Fisher, M. C., Henk, D. A., Briggs, C. J., Brownstein, J. S., Madoff, L. C., McCraw, S. L., and Gurr, S. J.: Emerging fungal threats to animal, plant and ecosystem health, Nature, 484, 186-194, 10.1038/nature10947, 2012.

Fröhlich-Nowoisky, J., Pickersgill, D. A., Desprès, V. R., and Pöschl, U.: High diversity of fungi in air particulate matter, Proceedings of the National Academy of Sciences, 106, 12814-12819, 10.1073/pnas.0811003106, 2009.

Froehlich-Nowoisky, J., Burrows, S. M., Xie, Z., Engling, G., Solomon, P. A., Fraser, M. P., Mayol-Bracero, O. L., Artaxo, P., Begerow, D., Conrad, R., Andreae, M. O., Despres, V. R., and

Poeschl, U.: Biogeography in the air: fungal diversity over land and oceans, Biogeosciences, 9, 1125-1136, 10.5194/bg-9-1125-2012, 2012.

Fuzzi, S., Mandrioli, P., and Perfetto, A.: Fog droplets - An atmospheric source of secondary biological aerosol particles, Atmospheric Environment, 31, 287-290, 10.1016/1352-2310(96)00160-4, 1997.

Gabey, A. M., Gallagher, M. W., Whitehead, J., Dorsey, J. R., Kaye, P. H., and Stanley, W. R.: Measurements and comparison of primary biological aerosol above and below a tropical forest canopy using a dual channel fluorescence spectrometer, Atmospheric Chemistry and Physics, 10, 4453-4466, 10.5194/acp-10-4453-2010, 2010.

Gabey, A. M., Stanley, W. R., Gallagher, M. W., and Kaye, P. H.: The fluorescence properties of aerosol larger than 0.8 mu m in urban and tropical rainforest locations, Atmospheric Chemistry and Physics, 11, 5491-5504, 10.5194/acp-11-5491-2011, 2011.

Gabey, A. M., Vaitilingom, M., Freney, E., Boulon, J., Sellegri, K., Gallagher, M. W., Crawford, I. P., Robinson, N. H., Stanley, W. R., and Kaye, P. H.: Observations of fluorescent and biological aerosol at a high-altitude site in central France, Atmospheric Chemistry and Physics, 13, 7415-7428, 10.5194/acp-13-7415-2013, 2013.

Gangamma, S.: Characteristics of airborne bacteria in Mumbai urban environment, Science of the Total Environment, 488, 70-74, 10.1016/j.scitotenv2014.04.065, 2014.

Garland, R. M., Schmid, O., Nowak, A., Achtert, P., Wiedensohler, A., Gunthe, S. S., Takegawa, N., Kita, K., Kondo, Y., Hu, M., Shao, M., Zeng, L. M., Zhu, T., Andreae, M. O., and Poschl, U.: Aerosol optical properties observed during Campaign of Air Quality Research in Beijing 2006 (CAREBeijing-2006): Characteristic differences between the inflow and outflow of Beijing city air, Journal of Geophysical Research-Atmospheres, 114, 2009.

Grand, L. F., and Vandyke, C. G.: Scanning electron microscopy of basidiospores of species of hydnellum, hydnum, phellodon, and bankera (hydnaceae), Journal of the Elisha Mitchell Scientific Society, 92, 114-123, 1976.

Hairston, P. P., Ho, J., and Quant, F. R.: Design of an instrument for real-time detection of bioaerosols using simultaneous measurement of particle aerodynamic size and intrinsic fluorescence, Journal of Aerosol Science, 28, 471-482, 10.1016/s0021-8502(96)00448-x, 1997.

Hallar, A. G., Chirokova, G., McCubbin, I., Painter, T. H., Wiedinmyer, C., and Dodson, C.: Atmospheric bioaerosols transported via dust storms in the western United States, Geophysical Research Letters, 38, 10.1029/2011gl048166, 2011.

Hameed, A. A. A., Khoder, M. I., Ibrahim, Y. H., Saeed, Y., Osman, M. E., and Ghanem, S.: Study on some factors affecting survivability of airborne fungi, Science of the Total Environment, 414, 696-700, 10.1016/j.scitotenv.2011.10.042, 2012.

Hameed, A. A. A., Khoder, M. I., Yuosra, S., Osman, A. M., and Ghanem, S.: Diurnal distribution of airborne bacteria and fungi in the atmosphere of Helwan area, Egypt, Science of the Total Environment, 407, 6217-6222, 10.1016/j.scitotenv.2009.08.028, 2009.

Hara, K., and Zhang, D.: Bacterial abundance and viability in long-range transported dust, Atmospheric Environment, 47, 20-25, 10.1016/j.atmosenv.2011.11.050, 2012.

Hasnain, S. M.: Influence of meteorological factors on the air spora, Grana, 32, 184-188, 1993.

Healy, D. A., Huffman, J. A., O'Connor, D. J., Poehlker, C., Poeschl, U., and Sodeau, J. R.: Ambient measurements of biological aerosol particles near Killarney, Ireland: a comparison between real-time fluorescence and microscopy techniques, Atmospheric Chemistry and Physics, 14, 8055-8069, 10.5194/acp-14-8055-2014, 2014.

Herrero, B., FombellaBlanco, M. A., FernandezGonzalez, D., and ValenciaBarrera, R. M.: The role of meteorological factors in determining the annual variation of Alternaria and Cladosporium snores in the atmosphere of Palencia, 1990-1992, International Journal of Biometeorology, 39, 139-142, 10.1007/bf01211226, 1996.

Hirst, J. M.: Changes in atmospheric spore content: Diurnal periodicity and the effects of weather, Transactions of the British Mycological Society, 36, 375-IN378, http://dx.doi.org/10.1016/S0007-1536(53)80034-3, 1953.

Hjelmroos, M.: Relationship between airborne fungal spore presence and weather variables - cladosporium and alternaria, Grana, 32, 40-47, 1993.

Ho, H. M., Rao, C. Y., Hsu, H. H., Chiu, Y. H., Liu, C. M., and Chao, H. J.: Characteristics and determinants of ambient fungal spores in Hualien, Taiwan, Atmospheric Environment, 39, 5839-5850, 10.1016/j.atmonsenv.2005.06.034, 2005.

Hollins, P. D., Kettlewell, P. S., Atkinson, M. D., Stephenson, D. B., Corden, J. M., Millington, W. M., and Mullins, J.: Relationships between airborne fungal spore concentration of Cladosporium and the summer climate at two sites in Britain, International Journal of Biometeorology, 48, 137-141, 10.1007/s00484-003-0188-9, 2004.

Horner, W. E., Oneil, C. E., and Lehrer, S. B.: Basidiospore aeroallergens, Clinical Reviews in Allergy, 10, 191-211, 1992.

Huffman, J. A., Treutlein, B., and Pöschl, U.: Fluorescent biological aerosol particle concentrations and size distributions measured with an Ultraviolet Aerodynamic Particle Sizer (UV-APS) in Central Europe, Atmos. Chem. Phys., 10, 3215-3233, 2010.

Huffman, J. A., Sinha, B., Garland, R. M., Snee-Pollmann, A., Gunthe, S. S., Artaxo, P., Martin, S. T., Andreae, M. O., and Poschl, U.: Size distributions and temporal variations of biological aerosol particles in the Amazon rainforest characterized by microscopy and real-time UV-APS fluorescence techniques during AMAZE-08, Atmospheric Chemistry and Physics, 12, 11997-12019, 10.5194/acp-12-11997-2012, 2012.

Huffman, J. A., Prenni, A. J., DeMott, P. J., Poehlker, C., Mason, R. H., Robinson, N. H., Froehlich-Nowoisky, J., Tobo, Y., Despres, V. R., Garcia, E., Gochis, D. J., Harris, E., Mueller-Germann, I., Ruzene, C., Schmer, B., Sinha, B., Day, D. A., Andreae, M. O., Jimenez, J. L., Gallagher, M., Kreidenweis, S. M., Bertram, A. K., and Poeschl, U.: High concentrations of biological aerosol particles and ice nuclei during and after rain, Atmospheric Chemistry and Physics, 13, 6151-6164, 10.5194/acp-13-6151-2013, 2013.

Jones, A. M., and Harrison, R. M.: The effects of meteorological factors on atmospheric bioaerosol concentrations - a review, Science of the Total Environment, 326, 151-180, 10.1016/j.scitotenv.2003.11.021, 2004.

Kanaani, H., Hargreaves, M., Ristovski, Z., and Morawska, L.: Performance assessment of UVAPS: Influence of fungal spore age and air exposure, Journal of Aerosol Science, 38, 83-96, 10.1016/j.jaerosci.2006.10.003, 2007.

Kanaani, H., Hargreaves, M., Smith, J., Ristovski, Z., Agranovski, V., and Morawska, L.: Performance of UVAPS with respect to detection of airborne fungi, Journal of Aerosol Science, 39, 175-189, 10.1016/j.jaerosci.2007.10.007, 2008.

Kanawade, V. P., Shika, S., Poehlker, C., Rose, D., Suman, M. N. S., Gadhavi, H., Kumar, A., Nagendra, S. M. S., Ravikrishna, R., Yu, H., Sahu, L. K., Jayaraman, A., Andreae, M. O., Poeschl, U., and Gunthe, S. S.: Infrequent occurrence of new particle formation at a semi-rural location, Gadanki, in tropical Southern India, Atmospheric Environment, 94, 264-273, 10.1016/j.atmosenv.2014.05.046, 2014.

Kurkela, T.: The number of Cladosporium conidia in the air in different weather conditions, Grana, 36, 54-61, 1997.

Lee, S.-H., Lee, H.-J., Kim, S.-J., Lee, H. M., Kang, H., and Kim, Y. P.: Identification of airborne bacterial and fungal community structures in an urban area by T-RFLP analysis and quantitative real-time PCR, Science of the Total Environment, 408, 1349-1357, 10.1016/j.scitotenv.2009.10.061, 2010.

Levetin, E., and Horner, W. E.: Fungal aerobiology: Exposure and measurement, Fungal Allergy and Pathogenicity, 81, 10-27, 2002.

Li, D. W., and Kendrick, B.: Functional-relationships between airborne fungal spores and environmental-factors in Kitchener-Waterloo, Ontario, as detected by canonical correspondence-analysis, Grana, 33, 166-176, 1994.

Li, F., and Ramanathan, V.: Winter to summer monsoon variation of aerosol optical depth over the tropical Indian Ocean, Journal of Geophysical Research-Atmospheres, 107, 10.1029/2001jd000949, 2002.

Li, M., Qi, J., Zhang, H., Huang, S., Li, L., and Gao, D.: Concentration and size distribution of bioaerosols in an outdoor environment in the Qingdao coastal region, Science of the Total Environment, 409, 3812-3819, 10.1016/j.scitotenv.2011.06.001, 2011.

Atmos. Chem. Phys. Discuss., doi:10.5194/acp-2016-265, 2016
Manuscript under review for journal Atmos. Chem. Phys.
Published: 8 April 2016

Lyon, F. L., Kramer, C. L., and Eversmeyer, M. G.: Variation of airspora in the atmosphere due to weather conditions, Grana, 23, 177-181, 1984.

Madden, L. V.: Effects of rain on splash dispersal of fungal pathogens, Canadian Journal of Plant Pathology, 19, 225-230, 1997.

Maki, T., Kakikawa, M., Kobayashi, F., Yamada, M., Matsuki, A., Hasegawa, H., and Iwasaka, Y.: Assessment of composition and origin of airborne bacteria in the free troposphere over Japan, Atmospheric Environment, 74, 73-82, 10.1016/j.atmosenv.2013.03.029, 2013.

Matthias-Maser, S., Obolkin, V., Khodzer, T., and Jaenicke, R.: Seasonal variation of primary biological aerosol particles in the remote continental region of Lake Baikal/Siberia, Atmospheric Environment, 34, 3805-3811, 10.1016/s1352-2310(00)00139-4, 2000.

Matthiasmaser, S., and Jaenicke, R.: A method to identify biological aerosol-particles with radius greater-than 0.3 μm for the determination of their size distribution, Journal of Aerosol Science, 22, S849-S852, 10.1016/s0021-8502(05)80232-0, 1991.

Matthiasmaser, S., and Jaenicke, R.: Examination of atmospheric bioaerosol particles with radii greater-than-0.2 μm, Journal of Aerosol Science, 25, 1605-1613, 10.1016/0021-8502(94)90228-3, 1994.

MatthiasMaser, S., and Jaenicke, R.: The size distribution of primary biological aerosol particles with radii >0.2 μm in an urban rural influenced region, Atmospheric Research, 39, 279-286, 10.1016/0169-8095(95)00017-8, 1995.

Moehler, O., DeMott, P. J., Vali, G., and Levin, Z.: Microbiology and atmospheric processes: the role of biological particles in cloud physics, Biogeosciences, 4, 1059-1071, 2007.

Moorthy, K. K., Nair, P. R., and Murthy, B. V. K.: Size distribution of coastal aerosols - effects of local-sources and sinks, Journal of Applied Meteorology, 30, 844-852, 10.1175/1520-0450(1991)030<0844:sdocae>2.0.co;2, 1991.

Morris, C. E., Georgakopoulos, D. G., and Sands, D. C.: Ice nucleation active bacteria and their potential role in precipitation, Journal De Physique Iv, 121, 87-103, 10.1051/jp4:2004121004, 2004.

Morris, C. E., Conen, F., Huffman, J. A., Phillips, V., Poeschl, U., and Sands, D. C.: Bioprecipitation: a feedback cycle linking Earth history, ecosystem dynamics and land use through biological ice nucleators in the atmosphere, Global Change Biology, 20, 341-351, 10.1111/gcb.12447, 2014.

Myers, N., Mittermeier, R. A., Mittermeier, C. G., da Fonseca, G. A. B., and Kent, J.: Biodiversity hotspots for conservation priorities, Nature, 403, 853-858, 10.1038/35002501, 2000.

Naja, M., and Lal, S.: Surface ozone and precursor gases at Gadanki (13.5 degrees N, 79.2 degrees E), a tropical rural site in India, Journal of Geophysical Research-Atmospheres, 107, 10.1029/2001jd000357, 2002.

Oh, J.-W., Lee, H.-B., Lee, H.-R., Pyun, B.-Y., Ahn, Y.-M., Kim, K.-E., Lee, S.-Y., and Lee, S.-I.: Aerobiological study of pollen and mold in Seoul, Korea, Allergology International, 47, 263-270, http://dx.doi.org/10.2332/allergolint.47.263, 1998.

Oliveira, M., Amorim, M. I., Ferreira, E., Delgado, L., and Abreu, I.: Main airborne Ascomycota spores: characterization by culture, spore morphology, ribosomal DNA sequences and enzymatic analysis, Applied Microbiology and Biotechnology, 86, 1171-1181, 10.1007/s00253-010-2448-z, 2010.

Pachauri, T., Singla, V., Satsangi, A., Lakhani, A., and Kumari, K. M.: Characterization of major pollution events (dust, haze, and two festival events) at Agra, India, Environmental Science and Pollution Research, 20, 5737-5752, 10.1007/s11356-013-1584-2, 2013.

Pan, Y. L., Holler, S., Chang, R. K., Hill, S. C., Pinnick, R. G., Niles, S., and Bottiger, J. R.: Single-shot fluorescence spectra of individual micrometer-sized bioaerosols illuminated by a 351- or a 266-nm ultraviolet laser, Optics Letters, 24, 116-118, 10.1364/ol.24.000116, 1999a.

Pan, Y. L., Holler, S., Chang, R. K., Hill, S. C., Pinnick, R. G., Niles, S., Bottiger, J. R., and Bronk, B. V.: Real-time detection and characterization of individual flowing airborne biological particles: fluorescence spectra and elastic scattering measurements, in: Air Monitoring and Detection of Chemical and Biological Agents Ii, edited by: Leonelli, J., and Althouse, M. L., Proceedings of the Society of Photo-Optical Instrumentation Engineers (Spie), 117-125, 1999b.

Poehlker, C., Huffman, J. A., and Poeschl, U.: Autofluorescence of atmospheric bioaerosols - fluorescent biomolecules and potential interferences, Atmospheric Measurement Techniques, 5, 37-71, 10.5194/amt-5-37-2012, 2012.

Poehlker, C., Huffman, J. A., Foerster, J. D., and Poeschl, U.: Autofluorescence of atmospheric bioaerosols: spectral fingerprints and taxonomic trends of pollen, Atmospheric Measurement Techniques, 6, 3369-3392, 10.5194/amt-6-3369-2013, 2013.

Poschl, U.: Atmospheric aerosols: Composition, transformation, climate and health effects, Angewandte Chemie-International Edition, 44, 7520-7540, 10.1002/anie.200501122, 2005.

Pöschl, U., Martin, S. T., Sinha, B., Chen, Q., Gunthe, S. S., Huffman, J. A., Borrmann, S., Farmer, D. K., Garland, R. M., Helas, G., Jimenez, J. L., King, S. M., Manzi, A., Mikhailov, E., Pauliquevis, T., Petters, M. D., Prenni, A. J., Roldin, P., Rose, D., Schneider, J., Su, H., Zorn, S. R., Artaxo, P., and Andreae, M. O.: Rainforest Aerosols as Biogenic Nuclei of Clouds and Precipitation in the Amazon, Science, 329, 1513-1516, 10.1126/science.1191056, 2010.

Pranesha, T. S., and Kamra, A. K.: Scavenging of aerosol particles by large water drops .2. The effect of electrical forces, Journal of Geophysical Research-Atmospheres, 102, 23937-23946, 10.1029/97jd01834, 1997a.

Pranesha, T. S., and Kamra, A. K.: Scavenging of aerosol particles by large water drops .3. Washout coefficients, half-lives, and rainfall depths, Journal of Geophysical Research-Atmospheres, 102, 23947-23953, 10.1029/97jd01835, 1997b.

Atmos. Chem. Phys. Discuss., doi:10.5194/acp-2016-265, 2016
Manuscript under review for journal Atmos. Chem. Phys.
Published: 8 April 2016

Atmospheric Chemistry and Physics Discussions

Prenni, A. J., Petters, M. D., Kreidenweis, S. M., Heald, C. L., Martin, S. T., Artaxo, P., Garland, R. M., Wollny, A. G., and Poschl, U.: Relative roles of biogenic emissions and Saharan dust as ice nuclei in the Amazon basin, Nature Geoscience, 2, 401-404, 2009.

Prenni, A. J., Tobo, Y., Garcia, E., DeMott, P. J., Huffman, J. A., McCluskey, C. S., Kreidenweis, S. M., Prenni, J. E., Poehlker, C., and Poeschl, U.: The impact of rain on ice nuclei populations at a forested site in Colorado, Geophysical Research Letters, 40, 227-231, 10.1029/2012gl053953, 2013.

Prospero, J. M.: Mineral and sea salt aerosol concentrations in various ocean regions, Journal of Geophysical Research-Oceans and Atmospheres, 84, 725-731, 10.1029/JC084iC02p00725, 1979.

Prospero, J. M., Blades, E., Mathison, G., and Naidu, R.: Interhemispheric transport of viable fungi and bacteria from Africa to the Caribbean with soil dust, Aerobiologia, 21, 1-19, 10.1007/s10453-004-5872-7, 2005.

Quintero, E., Rivera-Mariani, F., and Bolanos-Rosero, B.: Analysis of environmental factors and their effects on fungal spores in the atmosphere of a tropical urban area (San Juan, Puerto Rico), Aerobiologia, 26, 113-124, 10.1007/s10453-009-9148-0, 2010.

Raatikainen, T., Hyvarinen, A. P., Hatakka, J., Panwar, T. S., Hooda, R. K., Sharma, V. P., and Lihavainen, H.: The effect of boundary layer dynamics on aerosol properties at the Indo-Gangetic plains and at the foothills of the Himalayas, Atmospheric Environment, 89, 548-555, 10.1016/j.atmosenv.2014.02.058, 2014.

Radke, L. F., Hobbs, P. V., and Eltgroth, M. W.: Scavenging of aerosol-particles by precipitation, Journal of Applied Meteorology, 19, 715-722, 10.1175/1520-0450(1980)019<0715:soapbp>2.0.co;2, 1980.

Saari, S., Niemi, J. V., Ronkko, T., Kuuluvainen, H., Jarvinen, A., Pirjola, L., Aurela, M., Hillamo, R., and Keskinen, J.: Seasonal and Diurnal Variations of Fluorescent Bioaerosol Concentration and Size Distribution in the Urban Environment, Aerosol and Air Quality Research, 15, 572-581, 10.4209/aaqr.2014.10.0258, 2015.

Sabariego, S., de la Guardia, C. D., and Alba, F.: The effect of meteorological factors on the daily variation of airborne fungal spores in Granada (southern Spain), International Journal of Biometeorology, 44, 1-5, 10.1007/s004840050131, 2000.

Sadys, M., Skjoth, C. A., and Kennedy, R.: Back-trajectories show export of airborne fungal spores (Ganoderma sp.) from forests to agricultural and urban areas in England, Atmospheric Environment, 84, 88-99, 10.1016/j.atmosenv.2013.11.015, 2014.

Santarpia, J. L., Ratnesar-Shumate, S., Gilberry, J. U., and Quizon, J. J.: Relationship Between Biologically Fluorescent Aerosol and Local Meteorological Conditions, Aerosol Sci. Technol., 47, 655-661, 10.1080/02786826.2013.781263, 2013.

Satheesh, S. K., and Srinivasan, J.: Enhanced aerosol loading over Arabian Sea during the pre-monsoon season: Natural or anthropogenic?, Geophysical Research Letters, 29, 10.1029/2002gl015687, 2002.

Schumacher, C. J., Poehlker, C., Aalto, P., Hiltunen, V., Petaja, T., Kulmala, M., Poeschl, U., and Huffman, J. A.: Seasonal cycles of fluorescent biological aerosol particles in boreal and semi-arid forests of Finland and Colorado, Atmospheric Chemistry and Physics, 13, 11987-12001, 10.5194/acp-13-11987-2013, 2013.

Sesartic, A., and Dallafior, T. N.: Global fungal spore emissions, review and synthesis of literature data, Biogeosciences, 8, 1181-1192, 10.5194/bg-8-1181-2011, 2011.

Shaffer, B. T., and Lighthart, B.: Survey of culturable airborne bacteria at four diverse locations in Oregon: Urban, rural, forest, and coastal, Microbial Ecology, 34, 167-177, 10.1007/s002489900046, 1997.

Sharma, N. K., and Rai, A. K.: Allergenicity of airborne cyanobacteria Phormidium fragile and Nostoc muscorum, Ecotoxicology and Environmental Safety, 69, 158-162, 10.1016/j.ecoenv.2006.08.006, 2008.

Sherman, J. P., Sheridan, P. J., Ogren, J. A., Andrews, E., Hageman, D., Schmeisser, L., Jefferson, A., and Sharma, S.: A multi-year study of lower tropospheric aerosol variability and systematic relationships from four North American regions, Atmospheric Chemistry and Physics, 15, 12487-12517, 10.5194/acp-15-12487-2015, 2015.

Shika, S., et al.: Atmospheric aerosol properties at a semi-rural location in South India: particle size distributions and implications for cloud formation, to be submitted.

Sivaprakasam, V., Huston, A. L., Scotto, C., and Eversole, J. D.: Multiple UV wavelength excitation and fluorescence of bioaerosols, Optics Express, 12, 4457-4466, 10.1364/opex.12.004457, 2004.

Spracklen, D. V., and Heald, C. L.: The contribution of fungal spores and bacteria to regional and global aerosol number and ice nucleation immersion freezing rates, Atmospheric Chemistry and Physics, 14, 9051-9059, 10.5194/acp-14-9051-2014, 2014.

Srivastava, A., Singh, M., and Jain, V. K.: Identification and characterization of size-segregated bioaerosols at Jawaharlal Nehru University, New Delhi, Natural Hazards, 60, 485-499, 10.1007/s11069-011-0022-3, 2012.

Tarlo, S. M., Bell, B., Srinivasan, J., Dolovich, J., and Hargreave, F. E.: Human sensitization to ganoderma antigen, Journal of Allergy and Clinical Immunology, 64, 43-49, 10.1016/0091-6749(79)90082-4, 1979.

Tong, Y and Lighthart, B.: Diurnal Distribution of Total and Culturable Atmospheric Bacteria at a Rural Site, Aerosol Sci. Technol., 30, 246-254, 10.1080/027868299304822, 1999.

Toprak, E., and Schnaiter, M.: Fluorescent biological aerosol particles measured with the Waveband Integrated Bioaerosol Sensor WIBS-4: laboratory tests combined with a one year field study, Atmospheric Chemistry and Physics, 13, 225-243, 10.5194/acp-13-225-2013, 2013.

Trejo, M., Douarche, C., Bailleux, V., Poulard, C., Mariot, S., Regeard, C., and Raspaud, E.: Elasticity and wrinkled morphology of Bacillus subtilis pellicles, Proceedings of the National Academy of Sciences of the United States of America, 110, 2011-2016, 10.1073/pnas.1217178110, 2013.

Troutt, C., and Levetin, E.: Correlation of spring spore concentrations and meteorological conditions in Tulsa, Oklahoma, International Journal of Biometeorology, 45, 64-74, 10.1007/s004840100087, 2001.

Valsan, A. E., Priyamvada, H., Ravikrishna, R., Després, V. R., Biju, C. V., Sahu, L. K., Kumar, A., Verma, R. S., Philip, L., and Gunthe, S. S.: Morphological characteristics of bioaerosols from contrasting locations in southern tropical India – A case study, Atmospheric Environment, 122, 321-331, http://dx.doi.org/10.1016/j.atmosenv.2015.09.071, 2015.

Vinoj, V., and Satheesh, S. K.: Measurements of aerosol optical depth over Arabian Sea during summer monsoon season, Geophysical Research Letters, 30, 10.1029/2002gl016664, 2003.

Vinoj, V., Satheesh, S. K., and Moorthy, K. K.: Optical, radiative, and source characteristics of aerosols at Minicoy, a remote island in the southern Arabian Sea, Journal of Geophysical Research-Atmospheres, 115, 10.1029/2009jd011810, 2010.

Vinoj, V., Rasch, P. J., Wang, H., Yoon, J.-H., Ma, P.-L., Landu, K., and Singh, B.: Short-term modulation of Indian summer monsoon rainfall by West Asian dust, Nature Geoscience, 7, 308-313, 10.1038/ngeo2107, 2014.

Wang, C.-C., Fang, G.-C., and Lee, L.: Bioaerosols study in central Taiwan during summer season, Toxicology and Industrial Health, 23, 133-139, 10.1177/0748233707078741, 2007.

Yu, X., Wang, Z., Zhang, M., Kuhn, U., Xie, Z., Cheng, Y., Pöschl, U., and Su, H.: Ambient measurement of fluorescent aerosol particles with a WIBS in the Yangtze River Delta of China: potential impacts of combustion-generated aerosol particles, Atmos. Chem. Phys. Discuss., doi:10.5194/acp-2016-228, in review, 2016.

Zhang, T., Engling, G., Chan, C.-Y., Zhang, Y.-N., Zhang, Z.-S., Lin, M., Sang, X.-F., Li, Y. D., and Li, Y.-S.: Contribution of fungal spores to particulate matter in a tropical rainforest, Environmental Research Letters, 5, 10.1088/1748-9326/5/2/024010, 2010.

Atmos. Chem. Phys. Discuss., doi:10.5194/acp-2016-265, 2016
Manuscript under review for journal Atmos. Chem. Phys.
Published: 8 April 2016

Atmospheric Chemistry and Physics Discussions

Table 1: List of frequently used acronyms and symbols with units.

Symbol	Quantity, Unit
D_a	Aerodynamic diameter, µm
D_g	Geometric midpoint diameter of fluorescent particles
$D_{g,T}$	Geometric midpoint diameter of total particles
DNA	Deoxyribonucleic acid
FBAP	Fluorescent biological aerosol particle
He-Ne	Helium-Neon
ITCZ	Inter Tropical Convergence Zone
M_F	Integrated mass concentration of fluorescent particles, µg m^{-3}
M_T	Integrated mass concentration of total particles, µg m^{-3}
Nd:YAG	Neodymium-doped yttrium Aluminum garnet
NE	Northeast
N_F	Integrated number concentration of fluorescent particles, cm^{-3}
N_T	Integrated number concentration of total particles, cm^{-3}
PAH	Polycyclic aromatic hydrocarbon
PBAPs	Primary Biological Aerosol Particles
RH	Relative Humidity
SEM	Scanning Electron Microscopy
SW	Southwest
TAP	Total Aerosol Particle
TSP	Total Suspended Particle
UV-APS	Ultraviolet Aerodynamic Particle Sizer
λ	Wavelength, nm

Atmos. Chem. Phys. Discuss., doi:10.5194/acp-2016-265, 2016
Manuscript under review for journal Atmos. Chem. Phys.
Published: 8 April 2016

Atmospheric Chemistry and Physics Discussions
Open Access
EGU

Number		June	July	August	Campaign
N_T (cm^{-3})	Mean	2.66	1.54	0.96	1.77
	Median	2.45	1.48	0.73	1.44
N_F (cm^{-3})	Mean	0.03	0.007	0.015	0.017
	Median	0.02	0.006	0.007	0.01
N_F/N_T (%)	Mean	0.03	0.01	0.03	0.02
	Median	0.01		0.01	0.01
Mass		**June**	**July**	**August**	**Campaign**
M_T (µg m^{-3})	Mean	10.61	6.15	4.15	7.17
	Median	9.58	5.55	2.8	5.57
M_F (µg m^{-3})	Mean	0.42	0.11	0.18	0.24
	Median	0.33	0.09	0.1	0.15
M_F/M_T (%)	Mean	0.09	0.03	0.08	0.06
	Median	0.04	0.02	0.03	0.03

Table 2: Integrated number concentrations and mass concentrations of coarse TAP and FBAP (~1–20 µm): arithmetic mean and median for each month and for the entire measurement campaign

Atmos. Chem. Phys. Discuss., doi:10.5194/acp-2016-265, 2016
Manuscript under review for journal Atmos. Chem. Phys.
Published: 8 April 2016

Sl No:	Location	Land Use	Meaurement Period	Season	Instrument	FBAP Number Concentration	Total Number Concentration	Number Ratio (%)	Reference
1	Mainz, Central Europe	Semi-urban	Aug-Dec, 2006		UVAPS	3 x 10^{-2} cm^{-3}	1.05 cm^{-3}	4	Huffman et al., 2010
2	Central Amazonia rainforest	Tropical rainforest	Feb-Mar, 2008		UVAPS	7.3 x 10^{-2} cm^{-3}	0.33 cm^{-3}	24	Huffman et al., 2012
3	Manchester, UK	Urban	December, 2009		WIBS-3	2.9 x 10^{-4} cm^{-3} (FL1)	1.38 x 10^{-2} cm^{-3}	2.1	Gabey et al., 2011
						5.2 x 10^{-4} cm^{-3} (FL2)		3.7	
						1.1 x 10^{-5} cm^{-3} (FL3)		7.8	
4	Central France	Rural	22 Jun-3 July, 2010		WIBS-3	1.2 x 10^{-2} cm^{-3} (280 nm)			Gabey et al., 2013
						9.5 x 10^{-2} cm^{-3} (370 nm)			
5	Helinski, Finland	Urban	Feb, 2012 (Winter)	Winter	BioScout	1 x 10^{-2} cm^{-3}		23	Saari et al., 2015
			June-Aug, 2012 (Summer)	Summer		2.8 x 10^{-2} cm^{-3}		6	
				Summer	UVAPS	1.3 x 10^{-2} cm^{-3}		8	
6	Colarado, USA	Pine forest	June-July,2011	Dry period	WIBS-3			5.8	Crawford et al., 2014
				Wet Period	WIBS-4			15.2	
7	Finland	Rural forest	August,2009 - April,2011	Spring	UVAPS	1.5 x 10^{-2} cm^{-3}	0.43 cm^{-3}	4.4	Schumacher et al., 2013
				Summer		4.6 x 10^{-2} cm^{-3}	0.45 cm^{-3}	13	
				Fall		2.7 x 10^{-2} cm^{-3}	0.41 cm^{-3}	9.8	
				Winter		0.4 x 10^{-2} cm^{-3}	0.47 cm^{-3}	1.1	

Atmos. Chem. Phys. Discuss., doi:10.5194/acp-2016-265, 2016
Manuscript under review for journal Atmos. Chem. Phys.
Published: 8 April 2016

	Colorado , USA	Rural, semi-arid	2011-2012	Spring	UVAPS	1.5×10^{-2} cm^{-3}	0.73 cm^{-3}	2.5	
				Summer		3×10^{-2} cm^{-3}	0.44 cm^{-3}	8.8	
				Fall		1.7×10^{-2} cm^{-3}	0.28 cm^{-3}	5.7	
				Winter		0.53×10^{-2} cm^{-3}	0.2 cm^{-3}	3	
8	Karlsruhe, Germany	Semi-rural	April 2010 - April 2011		WIBS - 4	3.1×10^{-2} cm^{-3}	0.583 cm^{-3}	7.34	Toprak and Schnaiter., 2013
9	Nanjing, China	Sub-urban	Oct-Nov, 2013	Autumn	WIBS-4		13.1 cm^{-3}		Yu et al., 2016
						0.6 cm^{-3} (FL1)		4.6	
						3.4 cm^{-3} (FL2)		25.3	
						2.1 cm^{-3} (FL3)		15.6	

Table 3: Comparison with other online measurements carried out under various environmental conditions across the globe.

Atmos. Chem. Phys. Discuss., doi:10.5194/acp-2016-265, 2016
Manuscript under review for journal Atmos. Chem. Phys.
Published: 8 April 2016

Number		Dusty	Clean	HighBio
N_T (cm^{-3})	Mean	4.2	1.27	1.78
	Median	4.36	1.15	1.4
N_F(cm^{-3})	Mean	0.02	0.005	0.05
	Median	0.019	0.004	0.038
N_F/N_T	Mean	0.01	0.01	0.05
	Median			0.03
Mass		**Dusty**	**Clean**	**HighBio**
M_T (µg m^{-3})	Mean	16.34	5.12	7.7
	Median	16.84	4.28	5.85
M_F (µg m^{-3})	Mean	0.36	0.08	0.58
	Median	0.33	0.05	0.47
M_F/M_T	Mean	0.02	0.03	0.12
	Median	0.02	0.01	0.08

Table 4: Integrated number concentrations and mass concentrations of coarse TAP and FBAP (~1–20 µm): arithmetic mean and median for each focus period (Dusty, Clean and HighBio).

	Campaign			Dusty			Clean			High Bio		
	N_T	N_F	N_F/N_T	N_T	N_F	N_F/N_T	N_T	N_F	N_F/N_T	N_T	N_F	N_F/N_T
RH	-0.64	0.58	0.85	-0.25		0.18	-0.66	-0.01	0.13	-0.64	0.5	0.68
Temperature	0.45	-0.65	-0.82	0.34	-0.04	-0.25	0.78	0.02	-0.2	0.43	-0.68	-0.83
Wind Speed	0.4	-0.6	-0.78	0.09	-0.18	-0.31	-0.18	-0.27	0	0.3	-0.61	-0.74

Table 5: R^2 values for correlation between meteorological parameters (RH, Temperature and Wind Speed) and N_T, N_F and N_F/N_T during the entire campaign and each focus periods.

Atmos. Chem. Phys. Discuss., doi:10.5194/acp-2016-265, 2016
Manuscript under review for journal Atmos. Chem. Phys.
Published: 8 April 2016

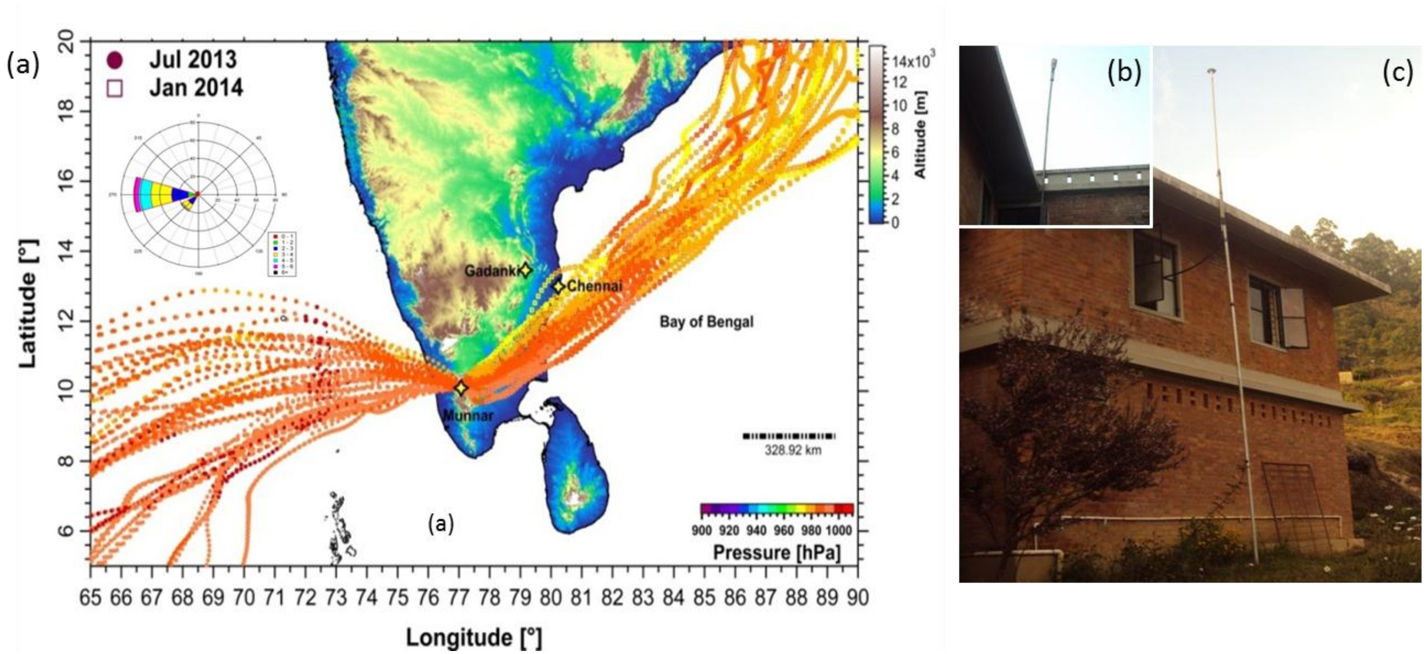

Figure 1: Location of measurement site Munnar (10.09°N, 77.06°E; 1605 m amsl – above mean sea level) located in the Western Ghat mountain range in Southern tropical India with 10 days back trajectories (HYSPLIT, NOAA-ARL GDAS1 model; start height 50 m above ground level; starting time 23:30 local time) illustrating the distinct and contrasting wind patterns during two contrasting seasons; Southwest monsoon season (representative month Jul) and Northeast monsoon season (representative month Jan) when field measurement campaign was carried out. It is evident that predominant wind pattern during Southwest monsoon season was Westerly/Southwesterly bringing the clean marine influx. Also shown in inset is wind rose diagram prepared using the data obtained using the ultrasonic weather station (a). The inlet system prepared for sampling the air using Ultraviolet Aerodynamic Particle Sizer (UV-APS) for bioaerosol number size distribution measurement. Inset shows the arrangement made for installing the ultrasonic weather station (b). The map shown is color-coded by topography (meters).

Atmos. Chem. Phys. Discuss., doi:10.5194/acp-2016-265, 2016
Manuscript under review for journal Atmos. Chem. Phys.
Published: 8 April 2016

Atmospheric Chemistry and Physics Discussions
Open Access

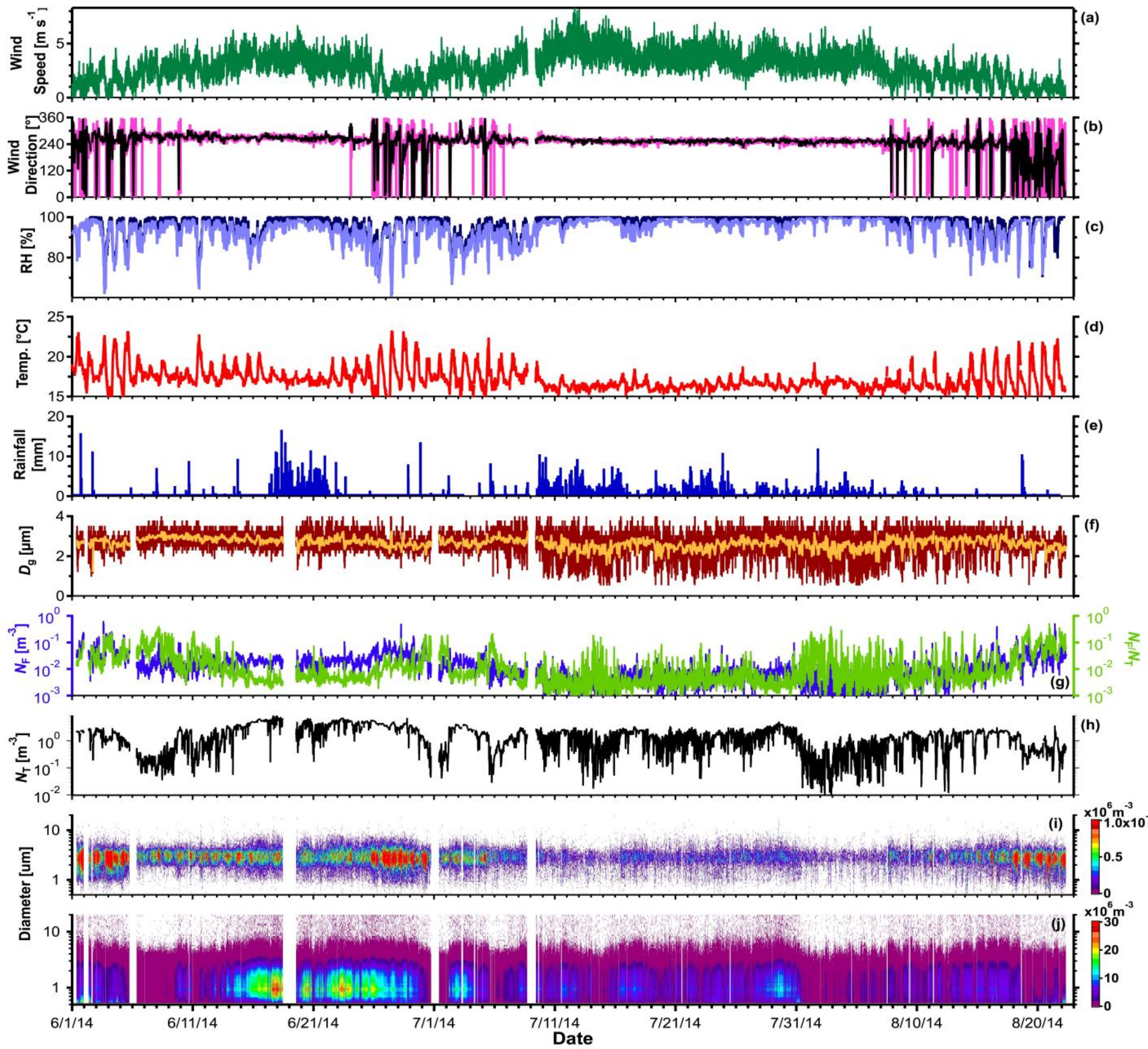

Figure 2: Time series of measured meteorological parameters, parameters derived from FBAP and total particle number size distribution measurements using UV-APS: (a) wind speed, (b) wind direction: five minutes average (magenta) and one hour average (black), (c) relative humidity, (d) temperature, (e) rainfall, (f) geometric mean diameter (D_g) five minutes average (dark red) and one hour average (yellow), (g) FBAP number concentration (N_F; blue) and relative contribution of FBAP to TAP (N_F/N_T; green), (h) TAP number concentration (N_T), (i) a contour plot of FBAP number size distribution (dN/dlog D_F), and (j) a contour plot of TAP number size distribution (dN/dlog D_T). The shadowed block represents the different focus periods (please refer to text for more details).

Atmos. Chem. Phys. Discuss., doi:10.5194/acp-2016-265, 2016
Manuscript under review for journal Atmos. Chem. Phys.
Published: 8 April 2016

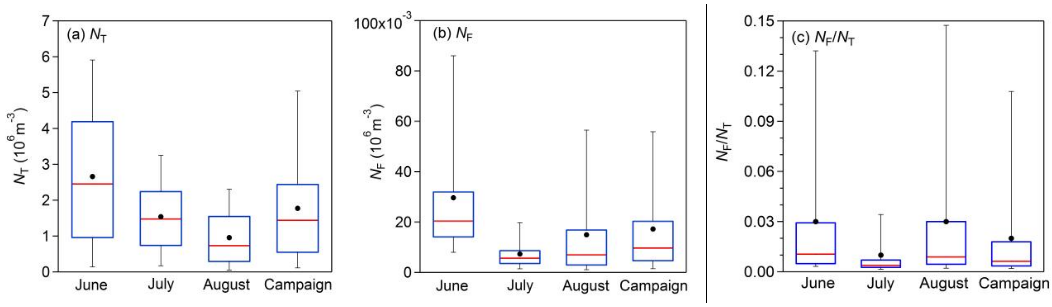

Figure 3: Statistical distribution of integrated (~1 – 20 µm) FBAP and TAP number and contribution of N_F to N_T measured during each month (Jun – Aug) of SW monsoon season and averaged over the entire measurement campaign carried out at Munnar as box whisker plots: (a) TAP number concentration (N_T), (b) FBAP number concentration (N_F), and (c) contribution of FBAP number concentration to TAP number concentration (N_F/N_T).

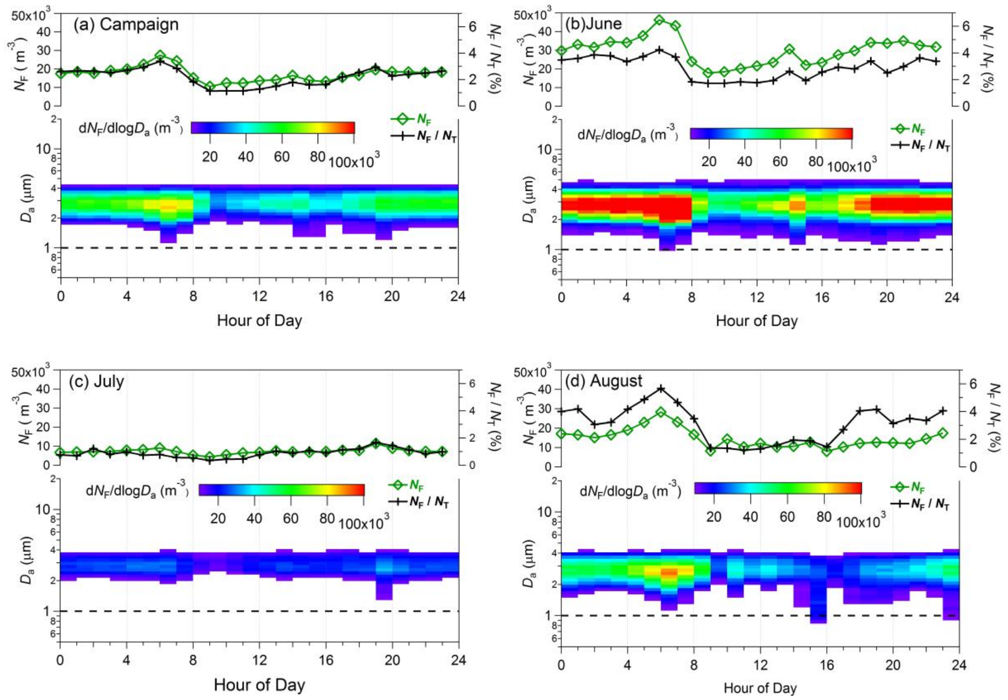

Figure 4: Diurnal cycles of FBAP number concentrations (N_F) and size distributions averaged over individual month of measurement and entire campaign (hourly median values plotted against the local time of the day). Upper portion of each panel shows integrated FBAP number concentration (~1 – 20 μm; N_F) on the left axis (green color) and FBAP fraction of TAP number (N_F/N_T) on the right axis (black color). Lower portion of each panel FBAP number size distribution (3-D plot) plotted against hour of the day on x-axis, aerodynamic diameter on y-axis and color is scaled for dN_F/dlog D_a indicates the concentration. Dashed black lines in lower portion of the each panel at 1.0 μm shows the particle size cut-off diameter below which fluorescent particles were not considered as FBAP due to potential interference with non-biological aerosol particles. (a) averaged over entire campaign,(b) Jun, (c) Jul, and (d) Aug. Please refer to supplementary Figs. for corresponding TAP plots.

Atmos. Chem. Phys. Discuss., doi:10.5194/acp-2016-265, 2016
Manuscript under review for journal Atmos. Chem. Phys.
Published: 8 April 2016

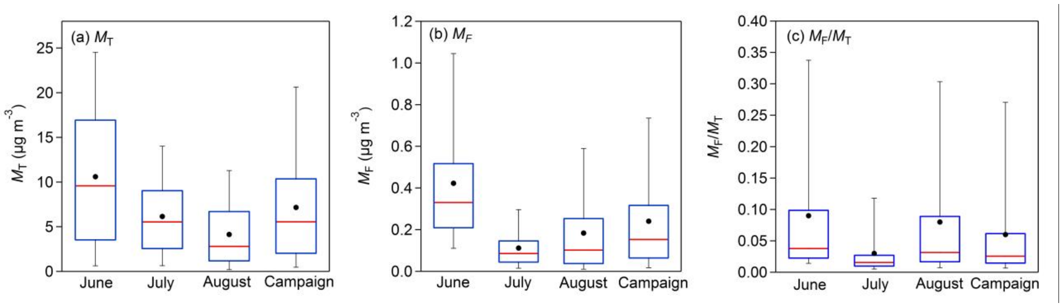

Figure 5: Same as Fig. 3 but for integrated (~1 – 20 μm) FBAP (M_F) and TAP (M_T) mass concentrations derived from number measurements by assuming unit density and shape factor.

Atmos. Chem. Phys. Discuss., doi:10.5194/acp-2016-265, 2016
Manuscript under review for journal Atmos. Chem. Phys.
Published: 8 April 2016

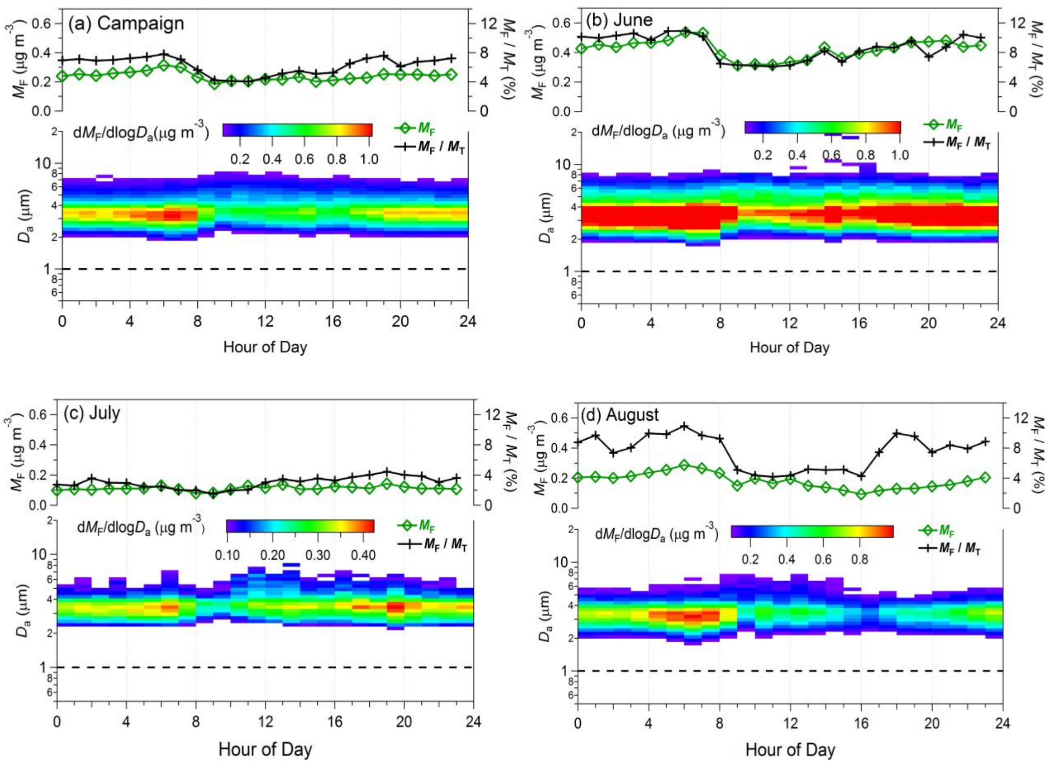

Figure 6: Same as Fig. 4 but representing the FBAP (M_F) mass concentrations.

Atmos. Chem. Phys. Discuss., doi:10.5194/acp-2016-265, 2016
Manuscript under review for journal Atmos. Chem. Phys.
Published: 8 April 2016

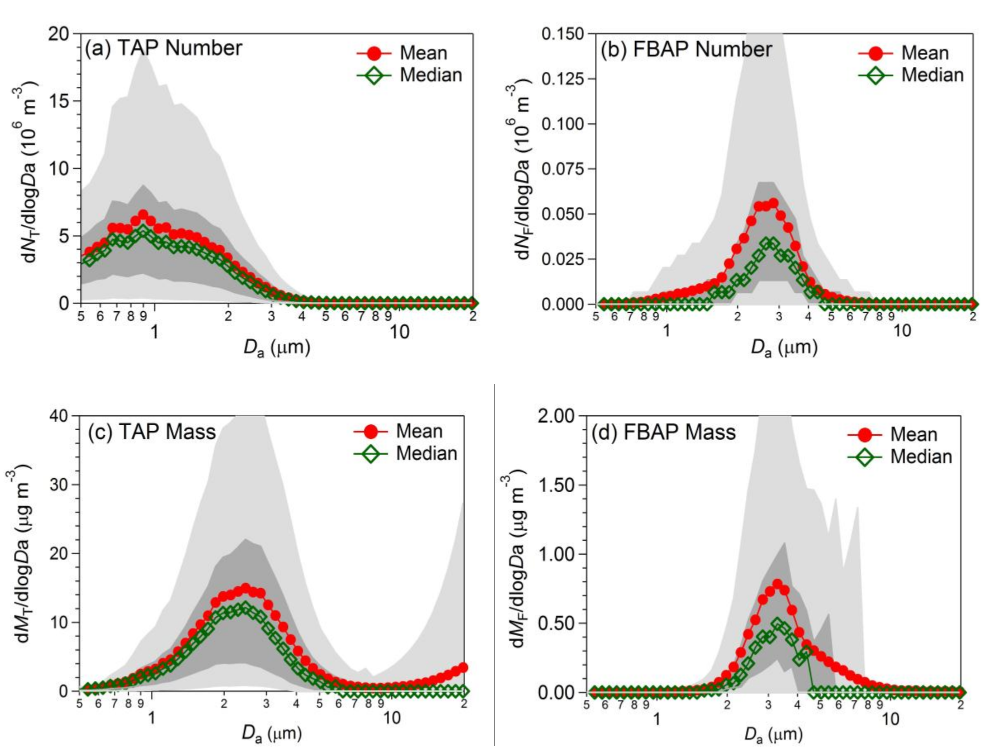

Figure 7: Particle number size and unit-normalized number size and mass size distributions averaged over the entire measurement campaign carried out at Munnar. Lower and upper parts of dark and light shaded area represents the 5th, 25th, 75th, and 95th percentile respectively. (a) TAP number (dN_T/dlog D_a), (b) FBAP number (dN_F/dlog D_a), (c) total mass (dM_T/dlog D_a), and (d) FBAP mass (dM_F/dlog D_a).

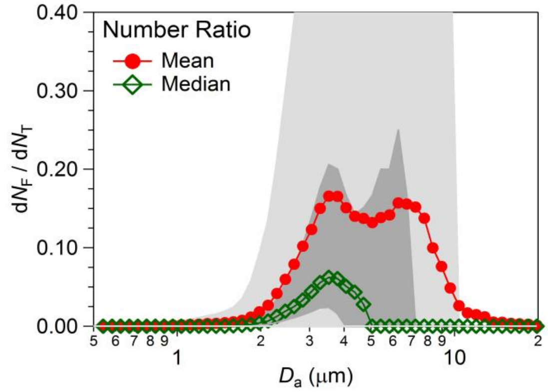

Figure 8: Size distribution of FBAP to TAP ratio averaged over the entire measurement period carried out at Munnar (dN_F/dlog D_a= dM_F/dlog D_a). Lower and upper parts of dark and light shaded area represents the 5th, 25th, 75th, and 95th percentile respectively.

Atmos. Chem. Phys. Discuss., doi:10.5194/acp-2016-265, 2016
Manuscript under review for journal Atmos. Chem. Phys.
Published: 8 April 2016

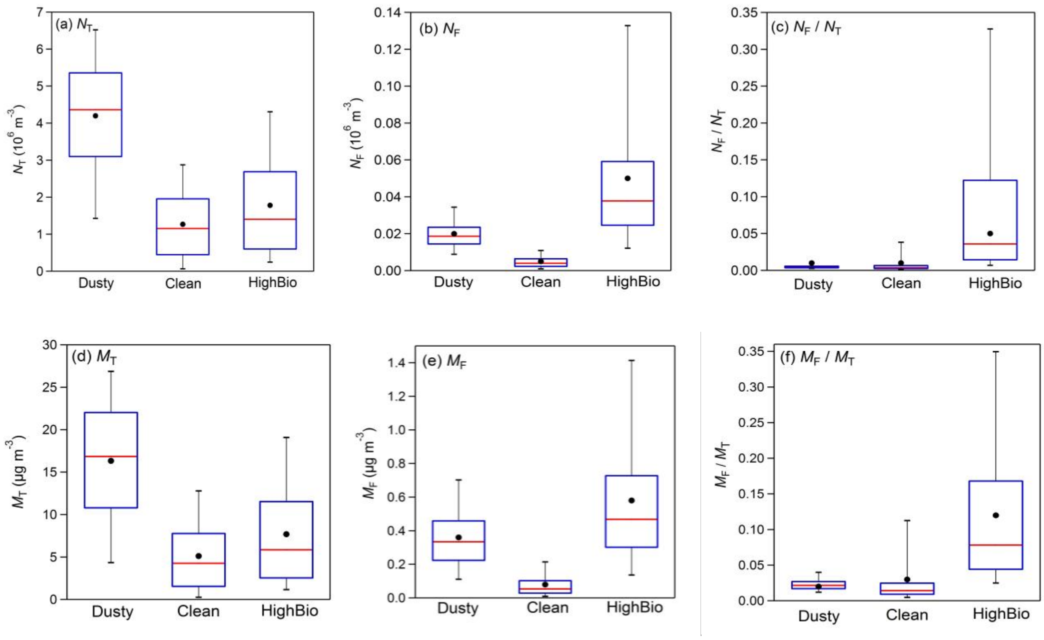

Figure 9: Statistical distribution of integrated (~1 – 20 µm) FBAP and TAP number and mass contribution of N_F to N_T, and M_F to M_T averaged over each distinct focus periods (dusty, clean, and high bio; please refer to the text for definitions related to each focus period) measurements carried out at Munnar as box whisker plots: (a) TAP number concentration (N_T), (b) FBAP number concentration (N_F), (c) contribution of FBAP number concentration to TAP number concentration (N_F/N_T), (d) TAP mass concentration (M_T), (e) FBAP mass concentration (M_F), and contribution of FBAP mass concentration to TAP mass concentration (M_T/M_F).

Atmos. Chem. Phys. Discuss., doi:10.5194/acp-2016-265, 2016
Manuscript under review for journal Atmos. Chem. Phys.
Published: 8 April 2016

Atmospheric Chemistry and Physics
Discussions

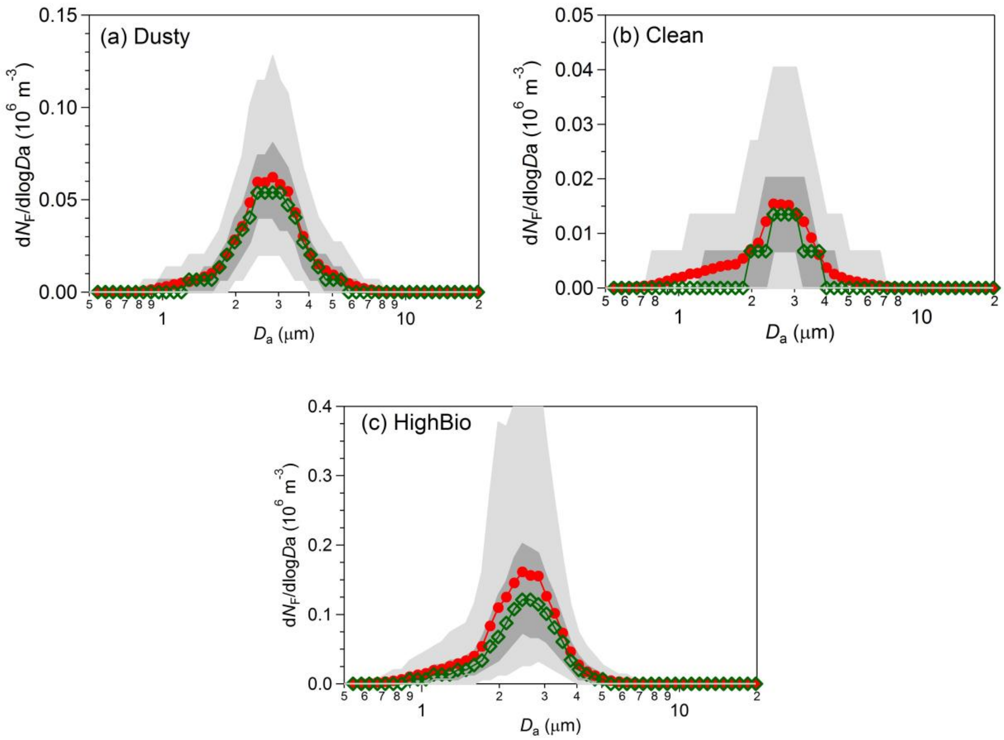

Figure 10: FBAP number size distributions ($dN_F/d\log D_a$) averaged over each distinct focus periods during the measurement campaign carried out at Munnar. Lower and upper parts of dark and light shaded area represents the 5th, 25th, 75th, and 95th percentile respectively. (a) dusty period , (b) clean period, and (c) high bio period.

Atmos. Chem. Phys. Discuss., doi:10.5194/acp-2016-265, 2016
Manuscript under review for journal Atmos. Chem. Phys.
Published: 8 April 2016

Atmospheric Chemistry and Physics
Discussions

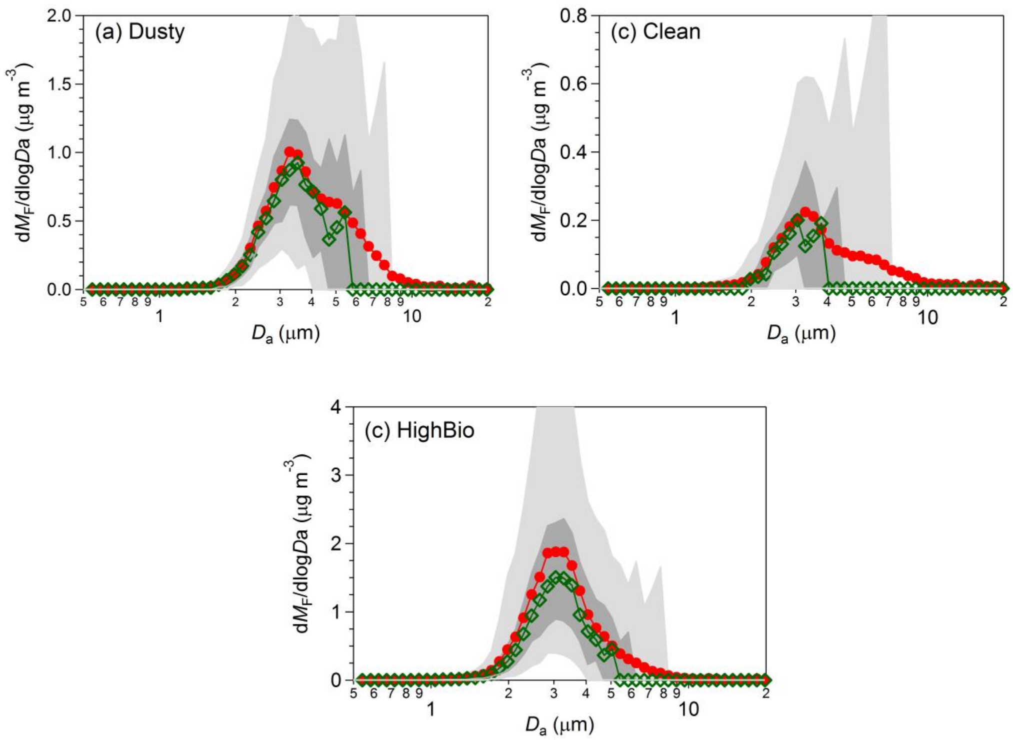

Figure 11: Same as Fig. 10 but representing FBAP mass size distribution (dM_F/dlog D_a).

Atmos. Chem. Phys. Discuss., doi:10.5194/acp-2016-265, 2016
Manuscript under review for journal Atmos. Chem. Phys.
Published: 8 April 2016

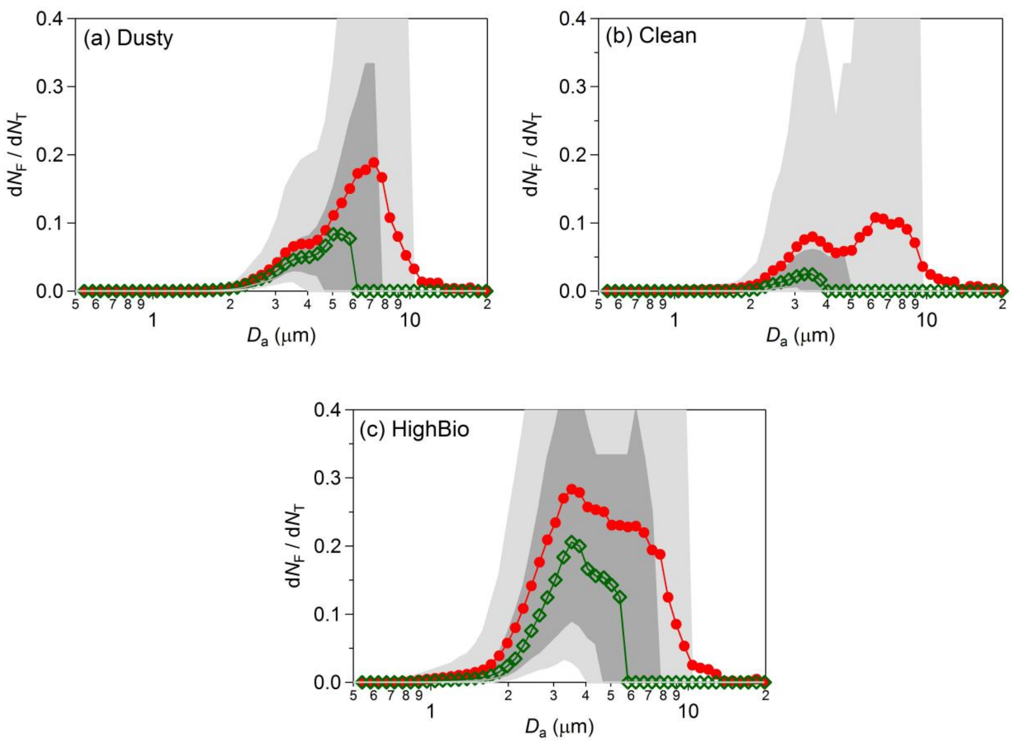

Figure 12: Size distribution of FBAP to TAP ratio averaged over the each distinct focus periods during the measurements carried out at Munnar (dN_F/dlog D_a= dM_F/dlog D_a). Lower and upper parts of dark and light shaded area represents the 5th, 25th, 75th, and 95th percentile respectively: (a) dusty, (b) clean, and (c) high bio.

Atmos. Chem. Phys. Discuss., doi:10.5194/acp-2016-265, 2016
Manuscript under review for journal Atmos. Chem. Phys.
Published: 8 April 2016

Atmospheric Chemistry and Physics
Discussions

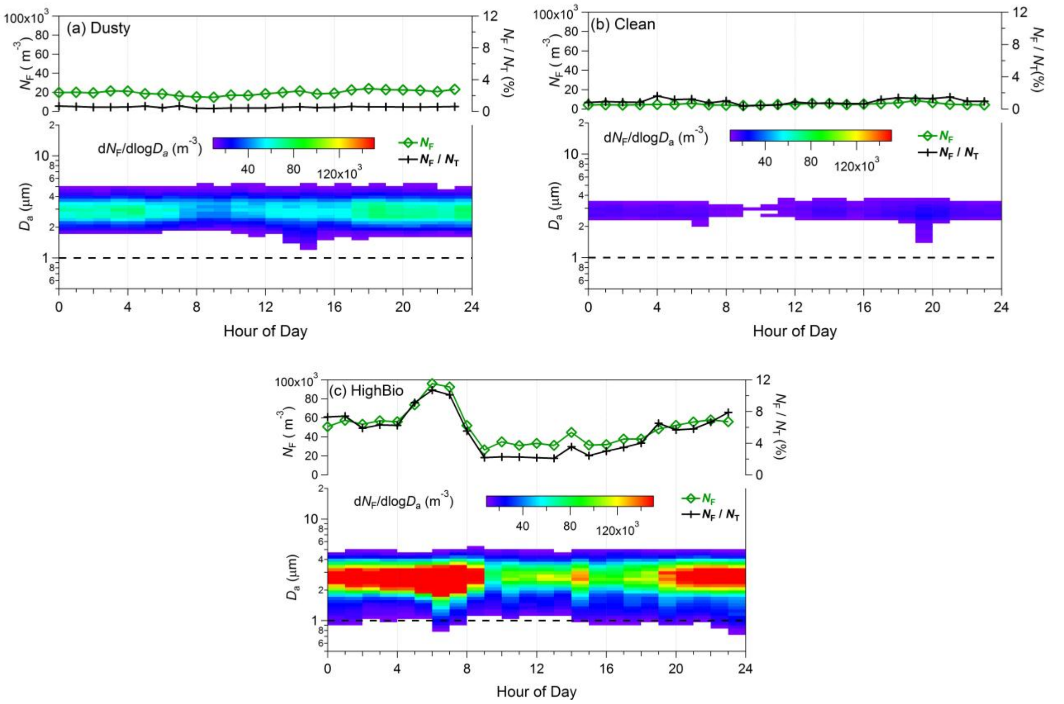

Figure 13: Diurnal cycles of FBAP number concentrations (N_F) and size distributions averaged over each distinct focus period identified during measurements carried out at Munnar (hourly median values plotted against the local time of the day). Upper portion of each panel shows integrated FBAP number concentration (~1 – 20 µm; N_F) on the left axis (green color) and FBAP fraction of TAP number (N_F/N_T) on the right axis (black color). Lower portion of each panel FBAP number size distribution (3-D plot) plotted against hour of the day on x-axis, aerodynamic diameter on y-axis and color is scaled for DN_F/dlog D_a indicates the concentration. Dashed black lines in lower portion of the each panel at 1.0 µm shows the particle size cut-off diameter below which fluorescent particles were not considered as FBAP due to potential interference with non-biological aerosol particles. (a) dusty (b) clean, and (c) high bio. Please refer to supplementary Figs. for corresponding TAP plots.

Atmos. Chem. Phys. Discuss., doi:10.5194/acp-2016-265, 2016
Manuscript under review for journal Atmos. Chem. Phys.
Published: 8 April 2016

Atmospheric Chemistry and Physics
Discussions

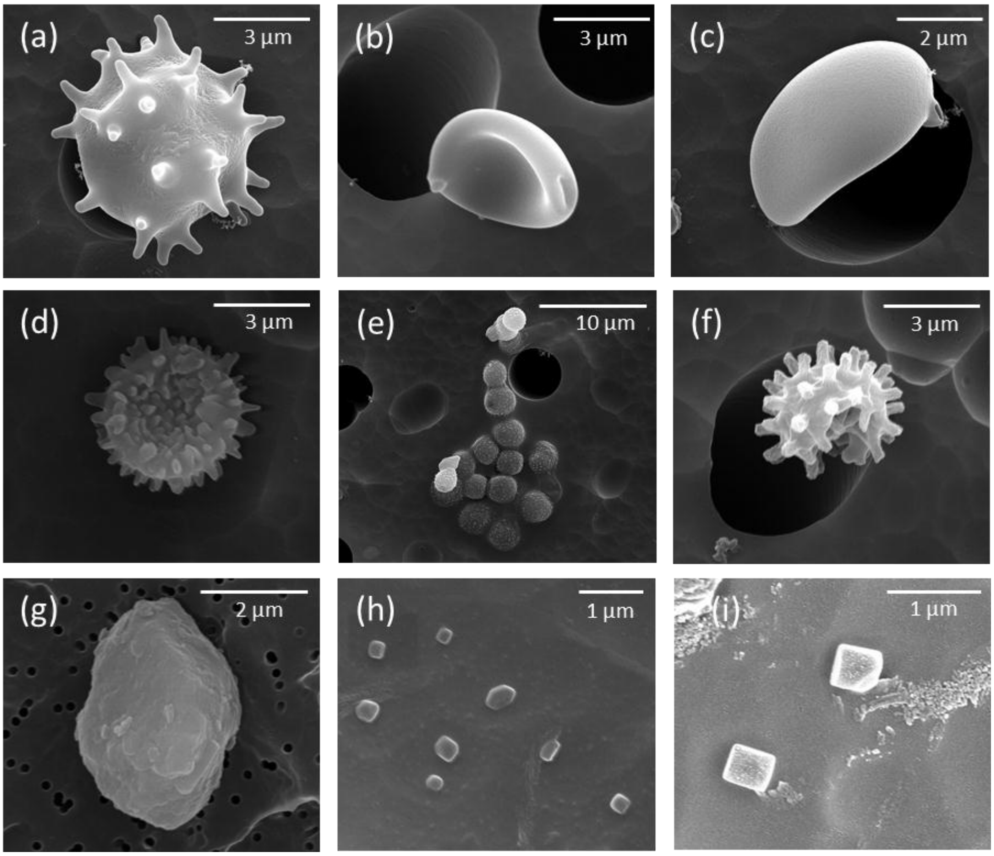

Figure 14: Scanning electron microscope images of the exemplary aerosol particles (FBAP and TAP) observed during the campaign at Munnar. The scale bar is shown at the top right corner of each image.

Atmos. Chem. Phys. Discuss., doi:10.5194/acp-2016-265, 2016
Manuscript under review for journal Atmos. Chem. Phys.
Published: 8 April 2016

Atmospheric Chemistry and Physics
Discussions

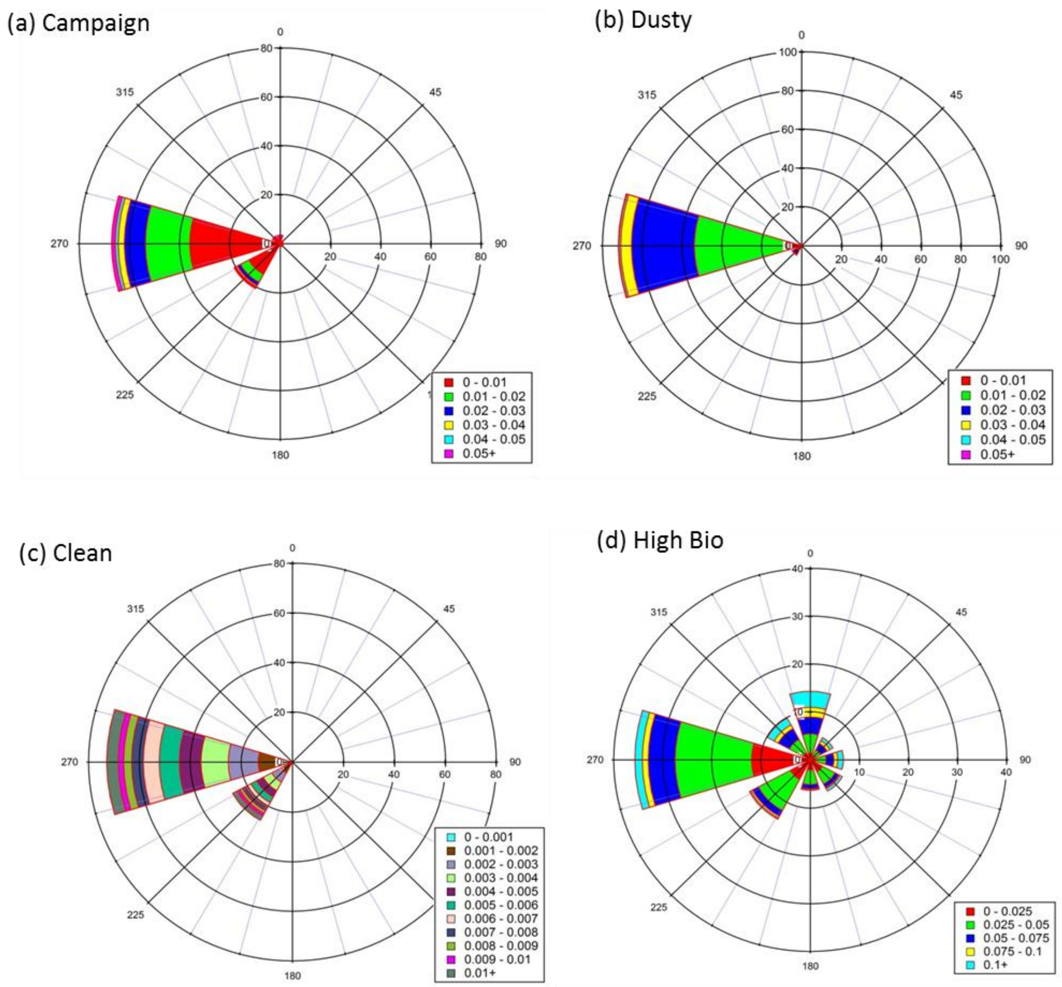

Figure 15: Wind rose diagram scaled over FBAP number concentration (N_F). These diagrams in a way are similar to the traditional wind rose diagram except representing the N_F in this case instead of wind speed. These diagram can be nominally interpreted as followed: For example (a) shows that ~52% of frequency of occurrence of N_F concentration in the range of 0 – 0.001 cm^{-3} was associated with Westerly/Southwesterly winds and on the contrary (d) indicates that out ~18% of frequency of occurrence of high concentration (N_F>0.1 cm^{-3}) ~16% was associated with Northerly/Northwesterly winds. (a) entire campaign, (b) dusty period, (c) clean period, and (d) high bio period.

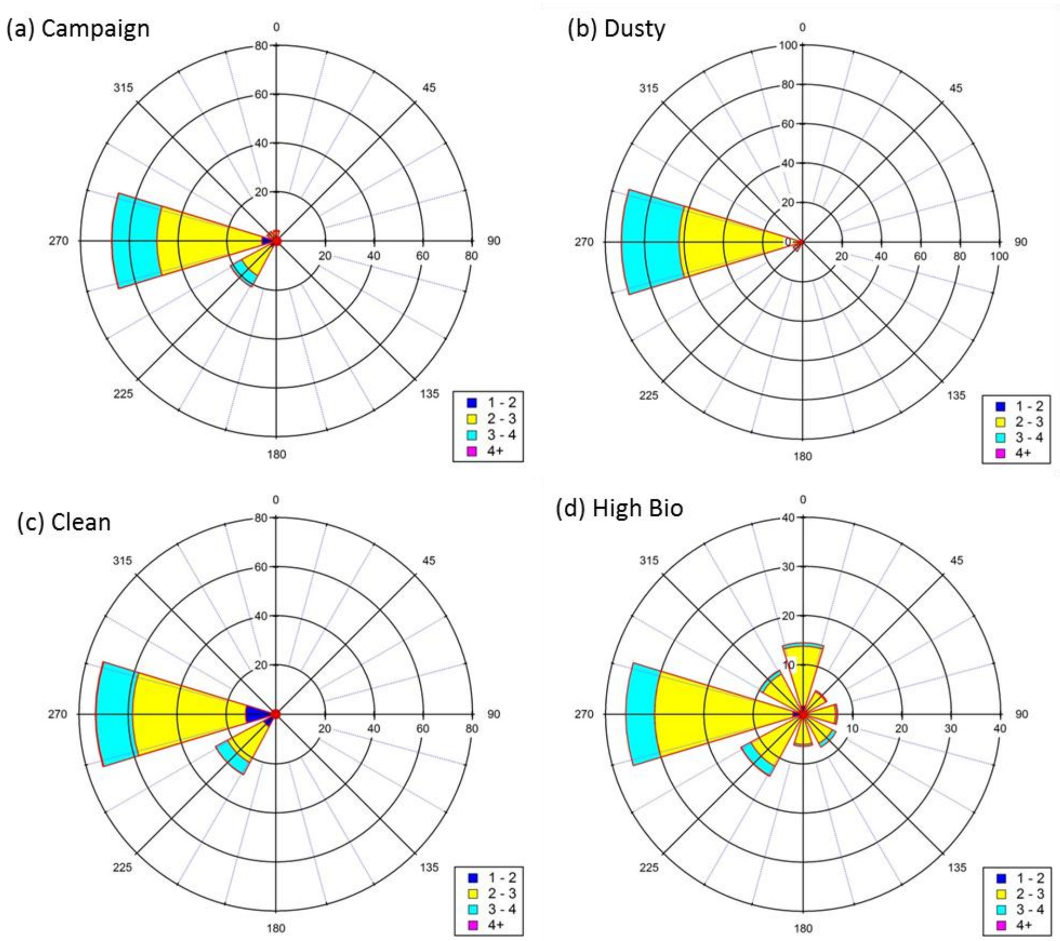

Figure 16: Same as Fig. 18 but scaled by geometric mean diameter (D_g) of dN_F/dlog D_a. (a) entire campaign, (b) dusty period, (c) clean period, and (d) high bio period.

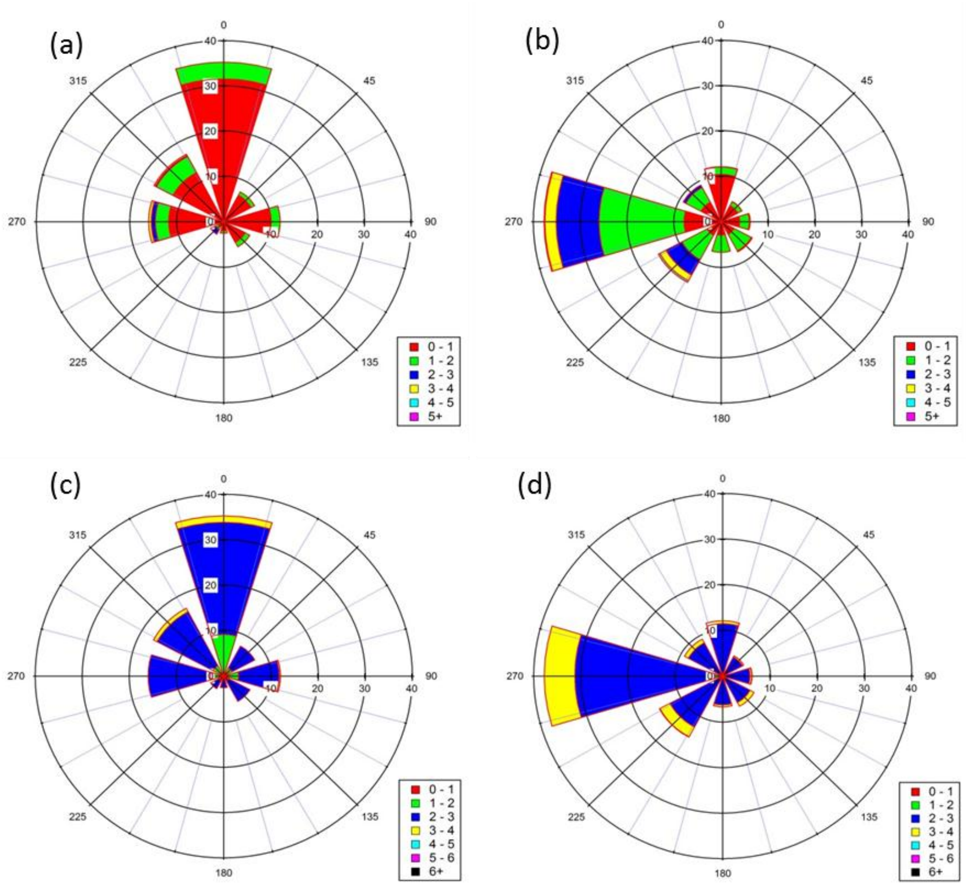

Figure 17: Wind rose diagram scaled by wind speed and geometric mean diameter (D_g) of dN_F/dlog D_a. The figures have been separated for FBAP number concentration (N_F) range, N_F >0.1 cm^{-3} and N_F< 0.1 cm^{-3} observed during high bio period. For example: when, N_F>0.1 cm^{-3} ~60% of the time wind was observed to be in the range of 0 – 1 m s^{-1} (a) and ~94% of the time the geometric mean diameter (D_g) of dN_F/dlog D_a was in the range of 2 – 3 μm (c). On the other hand for N_F<0.1 cm^{-3} ~60% of the time wind was greater than 1 m s^{-1} (b), and ~80% of the time geometric mean diameter (D_g) of dN_F/dlog D_a was in the range of 2 – 3 μm (d).

Atmos. Chem. Phys. Discuss., doi:10.5194/acp-2016-265, 2016
Manuscript under review for journal Atmos. Chem. Phys.
Published: 8 April 2016

Atmospheric Chemistry and Physics
Open Access
Discussions

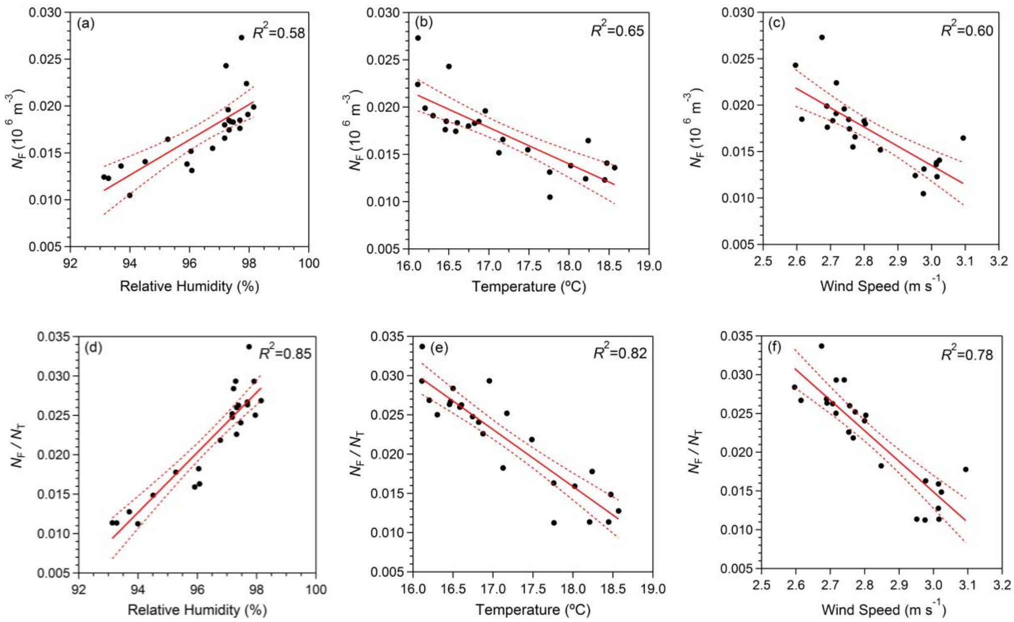

Figure 18: Correlation between aerosol particle number concentrations (N_F, N_T, and N_F/N_T) and meteorological parameters (relative humidity, temperature, and wind speed). Red line indicates the best fit to the scattered points and dashed black line indicates the 95% confidence level obtained for the best fit.